

Possible triply heavy tetraquark states in a chiral quark model

Xuejie Liu,^{1,*} Yue Tan,^{2,†} Dianyong Chen^{1,3,‡}, Hongxia Huang^{4,§} and Jialun Ping^{4,||}

¹*School of Physics, Southeast University, Nanjing 210094, People's Republic of China*

²*School of Mathematics and Physics, Yancheng Institute of Technology,
Yancheng 224051, People's Republic of China*

³*Lanzhou Center for Theoretical Physics, Lanzhou University,
Lanzhou 730000, People's Republic of China*

⁴*Department of Physics, Nanjing Normal University, Nanjing 210023, People's Republic of China*



(Received 11 December 2022; accepted 24 February 2023; published 13 March 2023)

In the present work, the triply heavy tetraquarks states $QQ\bar{Q}\bar{q}$ with $Q = (c, b)$ and $q = (u, d, s)$ with all possible quantum numbers are systematically investigated in the framework of the chiral quark model with the resonating ground method. Two kinds of structures, including the meson-meson configuration (the color-singlet channels and the hidden-color channels) and the diquark-antidiquark configuration (the color sextet-antisextet and the color triplet-antitriplet), are considered. In the considered system, several bound states are obtained for the $cc\bar{c}\bar{q}$, $bb\bar{c}\bar{q}$, and $bc\bar{c}\bar{q}$ tetraquarks. From the present estimations, we find that the coupled-channel effect is of great significance for forming below-threshold tetraquark states, which are stable for strong decays.

DOI: [10.1103/PhysRevD.107.054019](https://doi.org/10.1103/PhysRevD.107.054019)

I. INTRODUCTION

Searching for multi-quark states has become one of the most important and interesting topics of hadron physics, and the experimental observations and theoretical investigations shall deepen our understanding of the nonperturbative QCD [1–7]. At the early beginning of the quark model, the notion of multi-quark states had been proposed [8]. But there had been no progress on the experimental side for a long time. A turning point came in the year of 2003, when the Belle Collaboration reported their observation of a new charmoniumlike state $X(3872)$ in the exclusive $B^\pm \rightarrow K^\pm \pi^+ \pi^- J/\psi$ decays [9]. Since then, a growing number of new hadron states have been observed experimentally, which attract the great interest of experimentalists and theorists.

Among the new hadron states observed in the recent two decades, there are some good candidates of QCD exotic states, which can be classified into different categories

according to different criteria. For example, for the charmoniumlike states, we can divide them into two types according to the carried charges, i.e., the neutral and charged categories. One can also classify the new hadron states by their most possible quark components into tetraquark, pentaquark states, etc. It is interesting to notice that almost all the new hadron states have at least one heavy constituent quark or antiquark component. Since the mass of the heavy quarks is much larger than that of the light quarks, one can usually discuss the properties of hadrons with heavy quark components in the heavy quark limit. In this case, the number of heavy constituent quarks or antiquarks can also be used to classify the new hadron states. According to this criterion, we separate the observed new hadron states into three types, which are states with one, two, and four heavy quark or antiquark components, respectively. In the following, we select some typical examples for each type and present a short review.

- (i) *States with one heavy constituent quark or antiquark.*—The charmed-strange states $D_{s0}(2317)$ and $D_{s1}(2460)$ could be good examples of exotic states with one heavy constituent quark. In 2003, the BABAR Collaboration reported a narrow peak, named $D_{s0}(2317)$, in the $D_s^+ \pi^0$ invariant mass spectrum [10], and later this state was confirmed by the CLEO [11] and Belle [12] Collaborations. In addition to the $D_{s0}^*(2317)$, the CLEO Collaboration observed another narrow peak, named $D_{s1}(2460)$, in the $D_s^{*+} \pi^0$ invariant mass spectrum [11]. The J^P quantum numbers of the $D_{s0}^*(2317)$ and $D_{s1}(2460)$

*1830592517@qq.com

†tanyue@ycit.edu.cn

‡Corresponding author.
chendy@seu.edu.cn

§hxhuang@njnu.edu.cn

||jlping@njnu.edu.cn

Published by the American Physical Society under the terms of the [Creative Commons Attribution 4.0 International license](https://creativecommons.org/licenses/by/4.0/). Further distribution of this work must maintain attribution to the author(s) and the published article's title, journal citation, and DOI. Funded by SCOAP³.

indicated that they could be good candidates of 1^3P_0 and 1^3P_2 charmed-strange mesons [13–15]. However, the observed masses of $D_{s0}^*(2317)$ and $D_{s1}(2460)$ are much lower than the ones of the charmed-strange mesons predicted by the conventional quark model [16], which made the charmed-strange mesons assignments questionable. In addition, the masses of the $D_{s0}^*(2317)$ and $D_{s1}(2460)$ are just several tens of MeV below the thresholds of DK and D^*K ; thus, it was natural to interpret $D_{s0}^*(2317)$ and $D_{s1}(2460)$ as DK and D^*K molecular states [17–25], respectively. Moreover, these two states can also be assigned as $c\bar{s}q\bar{q}$ tetraquark states [26–31].

- (ii) *States with two heavy constituent quarks or antiquarks.*—As a typical example of exotic states with two heavy constituent quarks or antiquarks, $X(3872)$ is the first charmoniumlike state with the long-standing puzzle, which was observed in 2003 by the Belle Collaboration in the $\pi^+\pi^-J/\psi$ invariant mass distributions of the exclusive decay process $B^\pm \rightarrow K^\pm\pi^+\pi^-J/\psi$ [9] and then confirmed by CDF [32–35], D0 [36], BABAR [37–46], CMS [47–52], LHCb [53–66], and BESIII [67–70] in various processes. The $I(J^{PC})$ quantum numbers of $X(3872)$ have been determined to be $0(1^{++})$, which are well consistent with the ones of $\chi_{c1}(2P)$. Thus, in the literature, $X(3872)$ was interpreted as $\chi_{c1}(2P)$ charmonium [71–78]. However, the measured mass is much different with the expectation of the conventional quark model [79] but sandwiched by the thresholds of $D^0\bar{D}^{*0}$ and D^+D^{*-} . Moreover, the measured ratio of the branching fractions of $X(3872) \rightarrow \rho^0 J/\psi$ and $X(3872) \rightarrow \omega J/\psi$ indicated a large isospin violation [80], which is also inconsistent with conventional charmonium expectations. Thus, the charmonium interpretations became questionable, and some QCD exotic interpretations have been proposed, such as molecular [81–92] and tetraquark [93–106] interpretations.

- (iii) *States with four heavy constituent quarks or antiquarks.*—In 2020, the first tetraquark composed of four heavy constituent quarks or antiquarks, named $X(6900)$, was observed in the di- J/ψ invariant mass distributions [107]. Subsequently, this state was confirmed in the same channel by the CMS Collaboration [108], and then the existence of $X(6900)$ was verified by the ATLAS Collaboration in the di- J/ψ as well as $J/\psi\psi(2S)$ invariant mass distributions [109]. Besides $X(6900)$, some additional resonance states in this energy range have been reported, such as $X(6600)$ and $X(7200)$ by the CMS Collaboration [108] and $X(6200)$, $X(6600)$ as well as $X(7200)$ by the ATLAS Collaboration [109].

This recent experiment progress has inspired intensive theoretical investigations. The interpretations of their natures have been discussed extensively in compact tetraquark [110–116], $c\bar{c}$ hybrid [117], and Higgs-like boson [118] scenarios and the dynamical rescattering mechanism of double-charmonium channels as well [119–125].

The observations of the fully heavy tetraquark states makes tetraquark spectroscopy abundant and systematic. However, one can find that the tetraquark states with three heavy quark or antiquarks, i.e., $QQ\bar{Q}\bar{q}$ ($q = u, d, s$), are absent experimentally. The triply heavy tetraquark states are different from the already discovered quarkoniumlike states; it might in a sense offer a new platform of studying the internal structure of the exotic states. On the theoretical side, in the frame of color-magnetic interactions, the triply heavy tetraquark states were systematically investigated, and some exotic tetraquark states were predicted [126]. The QCD sum rule estimations indicated that the triply heavy tetraquarks states $cc\bar{c}\bar{q}$, $ccb\bar{q}$, and $bc\bar{b}\bar{q}$, with quantum numbers $J^P = 0^+$ and $J^P = 1^+$, are all heavier than the corresponding meson-meson thresholds, while the $bb\bar{b}\bar{q}$ tetraquarks were expected to be stable for strong decay [127]. However, the estimations in the extended chromomagnetic model [128], nonrelativistic quark model [129], and extended relativized quark model [130] indicated that there was no bound triply heavy tetraquark state. In a word, the existence of the triply heavy tetraquark states is still an open question. In the present work, we employ a nonrelativistic chiral quark model (ChQM) to estimate the mass spectra of the S -wave triply heavy tetraquark states with the possible J^P quantum numbers to be 0^+ , 1^+ , 2^+ , to further check the existence of triply heavy tetraquark states.

The work is organized as follows. In Secs. II and III, the theoretical framework utilized in present estimations is presented, which includes the chiral quark model and the resonating group method (RGM). Section IV is devoted to the analysis and discussion of the obtained results. In the last section, we give a short summary.

II. THE CHIRAL QUARK MODEL

In the quark model, the Hamiltonian of a hadron is generally written as [131]

$$H = \sum_{i=1}^4 \left(m_i + \frac{\mathbf{p}_i^2}{2m_i} \right) - T_{\text{c.m.}} + \sum_{j>i=1}^4 V(r_{ij}), \quad (1)$$

with m_i and p_i the mass and momentum of the i th quark, respectively. $T_{\text{c.m.}}$ is the center-of-mass kinetic energy, which is usually subtracted without losing generality, since one mainly focuses on the internal relative motions. $V(r_{ij})$ indicates the interaction potential between the i th and j th quarks.

As for the ChQM, it is constructed based on the fact that the light current quarks are nearly massless, which leads to chiral symmetry. However, due to the interactions of the quarks with the gluon medium, the current quarks become dressed, and such dressed current quarks can be approximately described by massive constituent quarks. In practice, the masses of the constituent quarks in the ChQM are determined by reproducing the spectrum of conventional hadrons, and this model has been widely used to investigate the study of the spectra of mesons containing heavy quarks [132–135], the electromagnetic, weak, and strong decays and reactions of mesons as well [135–140], and phenomena related to multiquark structures [141–147]. In addition, in the ChQM, the interaction potential usually includes the Goldstone-boson exchange potentials, the perturbative one-gluon interaction, and a confinement potential. Furthermore, when one considers only the S -wave tetraquark system, the spin-orbit and tensor contributions can be ignored; thus, the two-body interaction potential reads

$$V(r_{ij}) = V_{\text{OGE}}(r_{ij}) + V_{\chi}(r_{ij}) + V_{\text{CON}}(r_{ij}), \quad (2)$$

where $V_{\text{OGE}}(r_{ij})$ indicates the potential resulted from one-gluon exchange (OGE), and its concrete form is

$$V_{\text{OGE}}(r_{ij}) = \frac{1}{4} \alpha_s^{ij} \lambda_i^c \cdot \lambda_j^c \times \left[\frac{1}{r_{ij}} - \frac{\pi}{2} \delta(r_{ij}) \left(\frac{1}{m_i^2} + \frac{1}{m_j^2} + \frac{4\boldsymbol{\sigma}_i \cdot \boldsymbol{\sigma}_j}{3m_i m_j} \right) \right], \quad (3)$$

where $\boldsymbol{\sigma}$ and λ^c are the Pauli matrices and SU(3) color matrix, respectively. α_s^{ij} is the QCD-inspired scale-dependent quark-gluon coupling constant, which offers a consistent description of mesons from light- to heavy-quark sectors, and it can be determined by the mass splits between different mesons.¹ As for the confinement potential, the harmonic oscillator potential is adopted, which is

$$V_{\text{CON}}(r_{ij}) = -a_c \lambda_i^c \cdot \lambda_j^c [r_{ij}^2 + V_{0_{ij}}], \quad (4)$$

where a_c represents the strength of the confinement potential and $V_{0_{ij}}$ is the zero-point energies, which can be determined by the mass shift between different mesons.

The Goldstone-boson exchange interactions between light quarks appear because of the dynamical breaking of chiral symmetry. For the $QQ\bar{Q}\bar{q}$ with $Q = (c, b)$, $q = (u, d, s)$ systems, the π , K , and η exchange interactions do not work due to the quark components. Thus, in this

¹It worth mentioning that the $V_{\text{OGE}}(r_{ij}) \propto 1/r_{ij}$ is very singular at short range. Similar to the case of the hydrogen atom, the radial wave function should be proportional to r_{ij} for the S -wave state. Thus, the matrix elements of V_{OGE} are finite.

TABLE I. The concrete values of the model parameters, which are determined by reproducing the masses of mesons listed in Table II.

	Parameter	Value
Quark masses	m_u (MeV)	313
	m_s (MeV)	536
	m_c (MeV)	1728
	m_b (MeV)	5112
Confinement	b (fm)	0.2
	a_c (MeV fm ⁻²)	101
	$V_{0_{us}}$ (fm ²)	-3.7467
	$V_{0_{uc}}$ (fm ²)	-2.8684
	$V_{0_{ub}}$ (fm ²)	-2.6750
	$V_{0_{sc}}$ (fm ²)	-1.9211
	$V_{0_{sb}}$ (fm ²)	-1.7566
	$V_{0_{cc}}$ (fm ²)	-0.7367
	$V_{0_{cb}}$ (fm ²)	-1.0557
	$V_{0_{bb}}$ (fm ²)	2.6857
OGE	α_s^{us}	0.0716
	α_s^{uc}	0.1127
	α_s^{ub}	0.1057
	α_s^{sc}	0.1957
	α_s^{sb}	0.1930
	α_s^{cc}	0.4953
	α_s^{cb}	0.3241
	α_s^{bb}	2.3401

paper, the Goldstone-boson exchange interactions are not considered.

The concrete values of these parameters are collected in Table I. In addition, the details of how to obtain these parameters can also be found in Ref. [148]. The calculated meson masses in comparison with experimental values are shown in Table II. It should be noticed that the parameters in the potentials are obtained by reproducing the mass spectra of conventional mesons, but the two-body quark-quark interaction potentials could be extended to investigate the multiquark system, where the difference between the color configurations is reflected by the product of the SU(3) color matrix $\lambda_i^c \cdot \lambda_j^c$.

TABLE II. The masses (in units of MeV) of the mesons. The measured values of the masses [149] are also presented for comparison.

	K	K^*	B	B^*	B_s	B_s^*	B_c	B_c^*
Experiment	495	892	5280	5325	5366	5415	6275	...
Model	495	892	5280	5325	5366	5415	6275	6300
	η_b	Υ	D	D^*	D_s	D_s^*	η_c	J/ψ
Experiment	9398	9459	1865	2007	1968	2112	2984	3097
Model	9398	9459	1865	2007	1968	2112	2984	3097

III. THE RESONATING GROUP METHOD

In the present work, the triply heavy tetraquark systems are estimated by using the resonating group method [150]. In this method, the multi-quark system can be divided into two clusters, which are frozen inside, so one needs to consider only the relative motion between the two clusters. The conventional ansatz for two-cluster (clusters A and B) wave functions is

$$\psi_{4q} = \mathcal{A}[[\psi_A(\rho_A)\psi_B(\rho_B)]^{[\sigma]IS} \otimes \chi_L(\mathbf{R})]^J, \quad (5)$$

where \mathcal{A} is the antisymmetry operator of triply heavy tetraquarks.

For the $QQ\bar{Q}\bar{q}$ system, one has

$$\mathcal{A} = 1 - P_{13}. \quad (6)$$

This antisymmetry operator becomes

$$\mathcal{A} = 1 - P_{13} \quad (7)$$

for the $QQ\bar{Q}'\bar{q}$ system, and for the $QQ'\bar{Q}\bar{q}$ system, due to the absence of any homogeneous quarks, the antisymmetry operator becomes a unit operator, which is

$$\mathcal{A} = 1. \quad (8)$$

Moreover, $[\sigma] = [222]$ gives the total color symmetry, and $I, S, L,$ and J represent flavor, spin, orbital, and total angular momenta, respectively. ψ_A and ψ_B are the two-quark cluster wave functions, which are

$$\psi_A = \left(\frac{1}{2\pi b^2}\right)^{3/4} e^{-\rho_A^2/(4b^2)} \eta_{I_A} S_A \chi_A^c, \quad (9)$$

$$\psi_B = \left(\frac{1}{2\pi b^2}\right)^{3/4} e^{-\rho_B^2/(4b^2)} \eta_{I_B} S_B \chi_B^c, \quad (10)$$

where $\eta_I, S,$ and χ represent the flavor, spin, and internal color terms of the cluster wave functions, respectively. According to Fig. 1, we define different Jacobi coordinates for different diagrams. As for the meson-meson configuration in Fig. 1, the Jacobi coordinates are

$$\begin{aligned} \rho_A &= \mathbf{r}_{q_1} - \mathbf{r}_{\bar{q}_2}, & \rho_B &= \mathbf{r}_{q_3} - \mathbf{r}_{\bar{q}_4}, \\ \mathbf{R}_A &= \frac{m_1 \mathbf{r}_{q_1} + m_2 \mathbf{r}_{\bar{q}_2}}{m_1 + m_2}, \\ \mathbf{R}_B &= \frac{m_3 \mathbf{r}_{q_3} + m_4 \mathbf{r}_{\bar{q}_4}}{m_3 + m_4}, \\ \mathbf{R} &= \mathbf{R}_A - \mathbf{R}_B, \\ \mathbf{R}_c &= \frac{m_1 \mathbf{r}_{q_1} + m_2 \mathbf{r}_{\bar{q}_2} + m_3 \mathbf{r}_{q_3} + m_4 \mathbf{r}_{\bar{q}_4}}{m_1 + m_2 + m_3 + m_4}, \end{aligned} \quad (11)$$

where the subscript q (\bar{q}) indicates the quark (antiquark) particle, while the number indicates the quark position

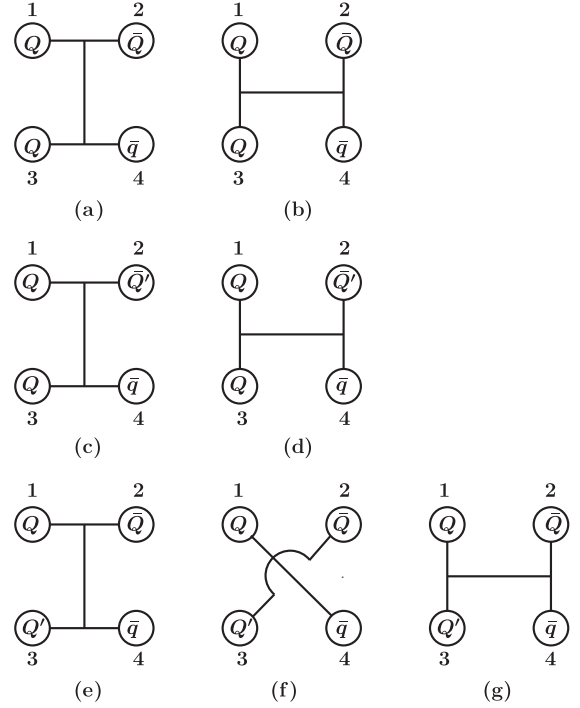


FIG. 1. Two types of configurations in $QQ\bar{Q}\bar{q}$, $QQ'\bar{Q}\bar{q}$, and $QQ\bar{Q}'\bar{q}$ tetraquarks. For the $QQ\bar{Q}\bar{q}$ system, there are two structures: the meson-meson configuration [diagram (a)] and the diquark-antidiquark configuration [diagram (b)]. For the $QQ'\bar{Q}\bar{q}$ system, diagrams (c) and (d) correspond to the meson-meson and the diquark-antidiquark configurations, respectively. For the $QQ'\bar{Q}\bar{q}$ system, diagrams (e) and (f) correspond to the meson-meson configuration, while diagram (g) refers to the diquark-antidiquark configuration.

in Fig. 1. By interchanging \mathbf{r}_{q_1} with \mathbf{r}_{q_3} , one can obtain the Jacobi coordinates in Fig. 1(f). As for the diquark-antidiquark configuration, one can also obtain the Jacobi coordinates corresponding to the diagrams in Fig. 1 by interchanging \mathbf{r}_{q_3} with $\mathbf{r}_{\bar{q}_2}$.

From the variational principle, after variation with respect to the relative motion wave function $\chi(\mathbf{R}) = \sum_L \chi_L(\mathbf{R})$, one obtains the RGM equation, which is

$$\int H(\mathbf{R}, \mathbf{R}') \chi(\mathbf{R}') d(\mathbf{R}') = E \int N(\mathbf{R}, \mathbf{R}') \chi(\mathbf{R}') d(\mathbf{R}'), \quad (12)$$

with $H(\mathbf{R}, \mathbf{R}')$ and $N(\mathbf{R}, \mathbf{R}')$ the Hamiltonian and normalization kernels, respectively. The eigenenergy E and the wave functions are obtained by solving the above RGM equation. In the present estimation, the function $\chi(\mathbf{R})$ can be expanded by Gaussian bases, which is

$$\begin{aligned} \chi(\mathbf{R}) &= \frac{1}{\sqrt{4\pi}} \sum_L \left(\frac{1}{\pi b^2}\right)^{3/4} \sum_i^n C_{i,L} \\ &\times \int e^{-\frac{1}{2}(R-S_i)^2/b^2} Y^L(\hat{S}_i) d\hat{S}_i, \end{aligned} \quad (13)$$

where $C_{i,L}$ is the expansion coefficient and n is the number of Gaussian bases, which is determined by the stability of the results. S_i is the separation of two reference centers. \mathbf{R} is the dynamic coordinate defined in Eq. (11). After including the motion of the center of mass, i.e.,

$$\phi_C(\mathbf{R}_c) = \left(\frac{4}{\pi b^2}\right)^{3/4} e^{-\frac{2R_c^2}{b^2}}. \quad (14)$$

With the above formula, one can rewrite the wave function in Eq. (5) as

$$\begin{aligned} \psi_{4q} = & \mathcal{A} \sum_{i,L} C_{i,L} \int \frac{d\hat{S}_i}{\sqrt{4\pi}} \prod_{\alpha=1}^2 \phi_\alpha(\mathbf{S}_i) \prod_{\alpha=3}^4 \phi_\beta(-\mathbf{S}_i) \\ & \times [[\eta_{I_A S_A} \eta_{I_B S_B}]^{IS} Y^L(\hat{S}_i)]^J [\chi_A^c \chi_B^c]^{[\sigma]}, \end{aligned} \quad (15)$$

where $\phi_\alpha(\mathbf{S}_i)$ and $\phi_\beta(-\mathbf{S}_i)$ are the single-particle orbital wave functions with different reference centers, which are

$$\begin{aligned} \phi_\alpha(\mathbf{S}_i) &= \left(\frac{1}{\pi b^2}\right)^{\frac{3}{4}} e^{-\frac{(r_{\alpha-\frac{1}{2}} S_i)^2}{2b^2}}, \\ \phi_\beta(-\mathbf{S}_i) &= \left(\frac{1}{\pi b^2}\right)^{\frac{3}{4}} e^{-\frac{(r_{\beta+\frac{1}{2}} S_i)^2}{2b^2}}. \end{aligned} \quad (16)$$

With the reformulated ansatz as shown in Eq. (15), the RGM equation becomes an algebraic eigenvalue equation, which is

$$\sum_{j,L} C_{j,L} H_{i,j}^{L,L'} = E \sum_j C_{j,L'} N_{i,j}^{L'}, \quad (17)$$

with $N_{i,j}^{L'}$ and $H_{i,j}^{L,L'}$ the overlap of the wave functions and the matrix elements of the Hamiltonian, respectively. By solving the generalized eigenvalue problem, we can obtain the energies of the tetraquark systems E and the corresponding expansion coefficient $C_{j,L}$. Finally, the relative motion wave function between two clusters can be obtained by substituting the $C_{j,L}$ into Eq. (13).

Besides the space part, we present the flavor, spin, and color parts of the wave function in the Appendix. It is worth noting that, after applying the antisymmetry operator, some wave functions may vanish, which means that some states are forbidden. For example, for the $cc\bar{b}\bar{q}$ system with $J^P = 0^+$, when considering the diquark-antidiquark structure with the spin wave function forced to choose S_0^1 , the color wave function χ_3^c would be excluded due to the constraints that the total wave function must be antisymmetric.

IV. RESULTS AND DISCUSSIONS

In the present calculation, the triply heavy tetraquark systems are evaluated by taking into account the

meson-meson and diquark-antidiquark configurations in the ChQM, which have been shown in Fig 1. To exhaust all possible configurations of the $QQ\bar{Q}\bar{q}$ systems, we divide them into three classes, which are the $QQ\bar{Q}\bar{q}$ system including $cc\bar{c}\bar{q}$ and $bb\bar{b}\bar{q}$, the $QQ\bar{Q}'\bar{q}$ system including $cc\bar{b}\bar{q}$ and $bb\bar{c}\bar{q}$, and the $QQ'\bar{Q}\bar{q}$ system including $cb\bar{b}\bar{q}$ and $cb\bar{c}\bar{q}$. Moreover, in the present work, only the S -wave triply heavy tetraquark states are evaluated, which indicates that the total orbital angular momenta L is equal to zero. Then, the total angular momentum J coincides with the total spin S and can take values of 0, 1, and 2, and the possible J^P quantum numbers of the tetraquark states could be 0^+ , 1^+ , and 2^+ . All the possible channels would be considered through the symmetry of the wave functions, and all the allowed channels are listed in Table III. From Table III, one can find that in the ChQM the color singlet-singlet ($1_c \times 1_c$) and the color octet-octet ($8_c \times 8_c$) structure have been taken into account for the meson-meson configuration. Moreover, for the diquark-antidiquark configuration, both antitriplet-triplet ($\bar{3}_c \times 3_c$) and sextet-antisextet ($6_c \times \bar{6}_c$) color structures have also been considered.

Our estimations of the eigenenergies of the triply tetraquark states are presented in Tables IV–XI. In these tables, all the allowed meson-meson and diquark-antidiquark configurations are listed. In the meson-meson channels, $(M_1 M_2)^1$ and $(M_1 M_2)^8$ indicate the color singlet-singlet ($1_c \times 1_c$) and the color octet-octet ($8_c \times 8_c$) structures, respectively. E_{th} is the experimental value of the

TABLE III. All the possible channels for different J^P quantum numbers, where $[i, j, k]$ denotes the channels with i, j , and k to be the indices of flavor, spin, and color, respectively.

$QQ\bar{Q}\bar{q}$		$QQ\bar{Q}'\bar{q}$		$QQ'\bar{Q}\bar{q}$			
J^P	Channel	J^P	Channel	J^P	Channel	J^P	Channel
0^+	[1, 1, 1]	0^+	[3, 1, 1]	0^+	[5, 1, 1]	1^+	[6, 3, 1]
	[1, 1, 2]		[3, 1, 2]		[5, 1, 2]		[6, 3, 2]
	[1, 2, 1]		[3, 2, 1]		[5, 2, 1]		[6, 4, 1]
	[1, 2, 2]		[3, 2, 2]		[5, 2, 2]		[6, 4, 2]
	[2, 1, 3]		[4, 1, 3]		[6, 1, 1]		[6, 5, 1]
	[2, 2, 4]		[4, 2, 4]		[6, 1, 2]		[6, 5, 2]
1^+	[1, 3, 1]	1^+	[3, 3, 1]	[6, 2, 1]	[7, 3, 3]		
	[1, 3, 2]		[3, 3, 2]	[6, 2, 2]	[7, 3, 4]		
	[1, 4, 1]		[3, 4, 1]	[7, 1, 3]	[7, 4, 3]		
	[1, 4, 2]		[3, 4, 2]	[7, 1, 4]	[7, 4, 4]		
	[1, 5, 1]		[3, 5, 1]	[7, 2, 3]	[7, 5, 3]		
	[1, 5, 2]		[3, 5, 2]	[7, 2, 4]	[7, 5, 4]		
	[2, 3, 3]		[4, 3, 3]	1^+	[5, 3, 1]	2^+	[5, 6, 1]
	[2, 4, 4]		[4, 4, 4]		[5, 3, 2]		[5, 6, 2]
	[2, 5, 4]		[4, 5, 4]		[5, 4, 1]		[6, 6, 1]
2^+	[1, 6, 1]	2^+	[3, 6, 1]	[5, 4, 2]	[6, 6, 2]		
	[1, 6, 2]		[3, 6, 2]	[5, 5, 1]	[7, 6, 3]		
	[2, 6, 4]		[4, 6, 4]	[5, 5, 2]	[7, 6, 4]		

thresholds for the physical channels. In the present work, the single-channel and channel-coupling calculations are all considered, and E_{sc} , E_{CC1} , E_{CC2} , and E_{CC} are the estimated values of the eigenenergies of every single channel, the coupled channel for the meson-meson configurations, the coupled channel for the diquark-antidiquark configurations, and the one estimated by simultaneously considering the meson-meson and diquark-antidiquark configurations, respectively. P indicates the percentages of each channel for the lowest-lying eigenenergies E_{CC} .

A. The $QQ\bar{Q}\bar{q}$ systems

Our estimations for the $cc\bar{c}\bar{q}$ tetraquark system are presented in Table IV. For the case of $J^P = 0^+$, one can find there are four channels in the meson-meson configurations and two channels in the diquark-antidiquark configurations. For the $cc\bar{c}\bar{n}$, $n = \{u, d\}$ tetraquark states, the lowest threshold of the physical channel is 4849 MeV, which is the threshold of $\eta_c D$. From the table, one can find that the eigenenergies of every single channel in both the meson-meson and diquark-antidiquark configurations are all above the lowest threshold of the allowed physics

channel, which indicates that all these tetraquark states can decay into $\eta_c D$. When one couples all the channels in a certain configuration, one can find that the estimated eigenenergies are 4851 and 5415 MeV for the meson-meson and diquark-antidiquark configurations, respectively, which is still a bit higher than the threshold of $\eta_c D$. After considering both the meson-meson and diquark-antidiquark configurations simultaneously, we find that the eigenenergy of the $cc\bar{c}\bar{n}$ tetraquark state is about 4851 MeV, which is about 2 MeV above the threshold of $\eta_c D$. As for $cc\bar{c}\bar{s}$ tetraquark states with $J^P = 0^+$, the lowest threshold of the physical channel is 4952 MeV, which is the threshold of $\eta_c D_s^+$. As for the $cc\bar{c}\bar{s}$ tetraquark state with $J^P = 0^+$, the single-channel estimations show that all the tetraquark states are heavier than $\eta_c D_s^+$. The eigenenergies of the coupled-channel estimations in meson-meson and diquark-antidiquark configurations are 4954 and 5487 MeV, respectively, which are all above the threshold of $\eta_c D_s^+$. Moreover, the full coupled-channel estimations, i.e., considering the meson-meson and diquark-antidiquark configurations simultaneously, indicate the eigenenergy of the $cc\bar{c}\bar{s}$ tetraquark state is

TABLE IV. The lowest-lying eigenenergies of the $cc\bar{c}\bar{n} = \{u, d\}$ and $cc\bar{c}\bar{s}$ tetraquarks in the ChQM.

J^P	$[i, j, k]$	$cc\bar{c}\bar{n}$				$cc\bar{c}\bar{s}$			
		Channel	E_{th}	E_{sc}	$P(\%)$	Channel	E_{th}	E_{sc}	$P(\%)$
0^+	[1, 1, 1]	$(\eta_c D)^1$	4849	4851	99.91	$(\eta_c D_s^+)^1$	4952	4954	99.98
	[1, 2, 1]	$(J/\psi D^*)^1$	5104	5106	0.01	$(J/\psi D_s^{*+})^1$	5209	5210	~ 0
	[1, 1, 2]	$(\eta_c D)^8$		5550	0.01	$(\eta_c D_s^+)^8$		5640	~ 0
	[1, 2, 2]	$(J/\psi D^*)^8$		5563	0.03	$(J/\psi D_s^{*+})^8$		5614	~ 0
	[2, 1, 3]	$(cc)(\bar{c}\bar{n})$		5624	0.01	$(cc)(\bar{c}\bar{s})$		5697	~ 0
	[2, 2, 4]	$(cc)(\bar{c}\bar{n})$		5421	0.03	$(cc)(\bar{c}\bar{s})$		5498	~ 0
		E_{CC1}		4851				4954	
		E_{CC2}		5415				5487	
		E_{CC}		4851				4954	
	1^+	[1, 3, 1]	$(\eta_c D^*)^1$	4991	4993	1.68	$(\eta_c D_s^{*+})^1$	5096	5098
[1, 4, 1]		$(J/\psi D)^1$	4962	4964	96.24	$(J/\psi D_s^+)^1$	5065	5067	99.91
[1, 5, 1]		$(J/\psi D^*)^1$	5104	5106	0.19	$(J/\psi D_s^{*+})^1$	5209	5211	~ 0
[1, 3, 2]		$(\eta_c D^*)^8$		5522	0.05	$(\eta_c D_s^{*+})^8$		5610	~ 0
[1, 4, 2]		$(J/\psi D)^8$		5526	0.09	$(J/\psi D_s^+)^8$		5614	~ 0
[1, 5, 2]		$(J/\psi D^*)^8$		5518	0.65	$(J/\psi D_s^{*+})^8$		5585	~ 0
[2, 3, 3]		$(cc)(\bar{c}\bar{n})$		5588	0.37	$(cc)(\bar{c}\bar{s})$		5661	~ 0
[2, 4, 4]		$(cc)(\bar{c}\bar{n})$		5364	0.06	$(cc)(\bar{c}\bar{s})$		5445	~ 0
[2, 5, 3]		$(cc)(\bar{c}\bar{n})$		5428	0.17	$(cc)(\bar{c}\bar{s})$		5508	~ 0
		E_{CC1}		4964				5067	
	E_{CC2}		5363				5442		
	E_{CC}		4963				5066		
2^+	[1, 6, 1]	$(J/\psi D^*)^1$	5104	5106	75.23	$(J/\psi D_s^{*+})^1$	5209	5211	99.79
	[1, 6, 2]	$(J/\psi D^*)^8$		5494	11.70	$(J/\psi D_s^{*+})^8$		5598	~ 0
	[2, 6, 4]	$(cc)(\bar{c}\bar{n})$		5442	13.06	$(cc)(\bar{c}\bar{s})$		5526	~ 0
		E_{CC1}		5106				5211	
		E_{CC2}		5442				5526	
	E_{CC}		5095				5211		

4594 MeV, which indicates that, in this case, the effects of channel coupling are rather weak. It is worth noting that in the single-channel estimation the eigenenergy for the lowest physical meson-meson channel is several hundred MeV below the ones of other channels; thus, in the coupled-channel estimations, the mixings between different channels are expected to be small due to the large eigenenergy splittings.

As for the $cc\bar{c}\bar{q}$ tetraquark system with $J^P = 1^+$, there are nine channels in this case, which include three color-singlet channels and three hidden-color channels in the meson-meson configuration, while there are three channels in the diquark-antidiquark configuration. The lowest physical meson-meson threshold is the one of $J/\psi D$, which is 4962 MeV. In the single-channel estimations, no bound state is found. The eigenenergies estimated in the coupled-channel estimations of the meson-meson and diquark-antidiquark configurations are 4964 and 5363 MeV, respectively, which are all above the threshold of $J/\psi D$. By considering both the meson-meson and diquark-antidiquark configurations simultaneously, the eigenenergy of the tetraquark state with $J^P = 1^+$ is estimated to be 4963 MeV, and the effect of the channel coupling is rather weak, which is similar to the case of $J^P = 0^+$. As for the $cc\bar{c}\bar{s}$ tetraquark system, the lowest physical threshold is the one of $J/\psi D_s^+$, which is 5065 MeV. Similar to the case of the $cc\bar{c}\bar{n}$ system, the eigenenergies obtained in the single channel are all above the threshold of $J/\psi D_s^+$. In addition, when we consider the channel coupling in the meson-meson and diquark-antidiquark configurations individually, the eigenenergies of the tetraquark state are estimated to be 5067 and 5442 MeV. After considering the meson-meson and diquark-antidiquark configurations simultaneously, we obtain that the eigenenergy of the $cc\bar{c}\bar{s}$ tetraquark state with $J^P = 1^+$ is 5066 MeV, which is still a bit higher than the threshold of $J/\psi D_s^+$.

For the case of $ccc\bar{n}$ tetraquark states with $J^P = 2^+$, there are two channels in the meson-meson configuration and only one channel in the diquark-antidiquark channel. The physical meson-meson threshold is 5104 MeV. Our single-channel estimations indicate that the eigenenergies are all above the threshold of $J/\psi D^*$, and, after considering the channel coupling in the meson-meson configuration, the eigenenergy is estimated to be 5106 MeV, which is still above the threshold of $J/\psi D^*$. When we include the meson-meson and diquark-antidiquark configuration simultaneously, the eigenenergy is estimated to be 5095 MeV, which is about 9 MeV below the threshold of $J/\psi D^*$, and then this tetraquark state cannot decay into $J/\psi D^*$. Moreover, our estimations indicate that in this state the dominant component is $J/\psi D^*$, which is about 75%, while the fractions of the hidden-color channel ($J/\psi D^*$)⁸ and the diquark-antidiquark channel (cc)($\bar{c}\bar{n}$) are about 11% and 13%, respectively, which indicate the effect of coupled channel plays an important role in the existence of

the below-threshold $cc\bar{c}\bar{n}$ tetraquark state. Different from the $cc\bar{c}\bar{n}$ system, our estimations find there are no below-threshold $cc\bar{c}\bar{s}$ tetraquark states with $J^P = 2^+$.

In a very similar way, we can estimate the $bb\bar{b}\bar{q}$ tetraquark system, and our results are listed in Table V. Our estimations indicate that there are no below-threshold $bb\bar{b}\bar{q}$ tetraquark states. However, within the framework of QCD sum rules, the $bb\bar{b}\bar{q}$ tetraquark states with $J^P = 0^+$ and $J^P = 1^+$ may be stable due to obtaining the masses below the threshold $\eta_b B$ and $\eta_b B^*$ [127], which is different from our conclusions. It is interesting to notice that, for the $cc\bar{c}\bar{n}$ system, we find one below-threshold tetraquark state with $J^P = 2^+$, while the mass of the corresponding state in the $bb\bar{b}\bar{n}$ sector is above the threshold of ΥB^* . To find which interaction plays the dominant role in forming a below-threshold $cc\bar{c}\bar{n}$ tetraquark state with $J^P = 2^+$ and further check the influence of the coupled-channel effect, we list the contribution of each term in the system Hamiltonian in Table VI. As we have discussed in the above section, the potential resulting from the Goldstone-boson exchange disappeared due to the quark components of the triply heavy tetraquark system. For the $cc\bar{c}\bar{n}$ tetraquark system with $J^P = 2^+$, $E_{M(J/\psi D^*)}$ refers to the sum of the theoretical threshold of $J/\psi D^*$, which indicates the interactions between J/ψ and D^* are zero and the system wave function is the product of the ones of J/ψ and D^* . In this case, the average value of the kinetic operator is 1800.1 MeV, and the ones of confinement and OGE terms are -1812.8 and -380.5 MeV, respectively; one can obtain the threshold of $J/\psi D^*$ by summing over the average values of different terms and the masses of the constituent quarks. In a similar way, one can obtain the average value of the operators in the single $E_{(J/\psi D^*)^1}$ channel estimation, the coupled-channel estimations of meson-meson configuration (E_{cc1}) and diquark-antidiquark configuration E_{cc2} , and the coupled-channel estimation of both meson-meson and diquark-antidiquark configurations E_{cc} . To simplify, we can define the ΔE as the difference of the average values of operators between single- and coupled-channel cases and $E_{M(J/\psi D^*)}$. If the sum of ΔE for all the operators is negative, the tetraquark states are below the threshold of $J/\psi D^*$. From the table, one can find the sum of ΔE for a single channel, the coupled channel of each configuration is positive, while the coupled channel of both configurations is negative, which indicates the $cc\bar{c}\bar{n}$ tetraquark state with $J^P = 2^+$ is a below-threshold state and the coupled-channel effects between different configurations are essential in forming a below-threshold tetraquark state. From the table, this result is mainly due to the strong attraction of the interaction of the OGE term under the coupling of all configurations. As for the $bb\bar{b}\bar{n}$ tetraquark state with $J^P = 2^+$, one can find that all the ΔE are positive, which indicates the tetraquark state is above the threshold of ΥB^* .

TABLE V. The lowest-lying eigenenergies of the $bb\bar{b}\bar{n}$ $n = \{u, d\}$ and $bb\bar{b}\bar{s}$ tetraquarks in the ChQM.

J^P	$[i, j, k]$	$bb\bar{b}\bar{n}$				$bb\bar{b}\bar{s}$			
		Channel	E_{th}	E_{sc}	$P(\%)$	Channel	E_{th}	E_{sc}	$P(\%)$
0^+	[1, 1, 1]	$(\eta_b\bar{B})^1$	14679	14681	99.99	$(\eta_b\bar{B}_s)^1$	14766	14767	99.99
	[1, 2, 1]	$(\Upsilon\bar{B}^*)^1$	14785	14787	0.01	$(\Upsilon\bar{B}_s^*)^1$	14875	14876	~ 0
	[1, 1, 2]	$(\eta_b\bar{B})^8$		15302	~ 0	$(\eta_b\bar{B}_s)^8$		15315	~ 0
	[1, 2, 2]	$(\Upsilon\bar{B}^*)^8$		15342	~ 0	$(\Upsilon\bar{B}_s^*)^8$		15327	~ 0
	[2, 1, 3]	$(bb)(\bar{b}\bar{n})$		15359	~ 0	$(bb)(\bar{b}\bar{s})$		15358	~ 0
	[2, 2, 4]	$(bb)(\bar{b}\bar{n})$		15144	~ 0	$(bb)(\bar{b}\bar{s})$		15171	~ 0
		E_{CC1}		14681				14767	
		E_{CC2}		15143				15170	
		E_{CC}		14680				14767	
	1^+	[1, 3, 1]	$(\eta_b\bar{B}^*)^1$	14724	14726	99.98	$(\eta_b\bar{B}_s^*)^1$	14814	14815
[1, 4, 1]		$(\Upsilon\bar{B})^1$	14740	14742	0.01	$(\Upsilon\bar{B}_s)^1$	14827	14828	~ 0
[1, 5, 1]		$(\Upsilon\bar{B}^*)^1$	14785	14787	0.01	$(\Upsilon\bar{B}_s^*)^1$	14875	14876	~ 0
[1, 3, 2]		$(\eta_b\bar{B}^*)^8$		15292	~ 0	$(\eta_b\bar{B}_s^*)^8$		15304	~ 0
[1, 4, 2]		$(\Upsilon\bar{B})^8$		15294	~ 0	$(\Upsilon\bar{B}_s)^8$		15307	~ 0
[1, 5, 2]		$(\Upsilon\bar{B}^*)^8$		15306	~ 0	$(\Upsilon\bar{B}_s^*)^8$		15304	~ 0
[2, 3, 3]		$(bb)(\bar{b}\bar{n})$		15348	~ 0	$(bb)(\bar{b}\bar{s})$		15346	~ 0
[2, 4, 4]		$(bb)(\bar{b}\bar{n})$		15127	~ 0	$(bb)(\bar{b}\bar{s})$		15155	~ 0
[2, 5, 3]		$(bb)(\bar{b}\bar{n})$		15147	~ 0	$(bb)(\bar{b}\bar{s})$		15175	~ 0
		E_{CC1}		14726				14815	
	E_{CC2}		15127				15155		
	E_{CC}		14726				14815		
2^+	[1, 6, 1]	$(\Upsilon\bar{B}^*)^1$	14785	14787	99.99	$(\Upsilon\bar{B}_s^*)^1$	14875	14876	99.99
	[1, 6, 2]	$(\Upsilon\bar{B}^*)^8$		15273	~ 0	$(\Upsilon\bar{B}_s^*)^8$		15298	~ 0
	[2, 6, 4]	$(bb)(\bar{b}\bar{n})$		15153	0.01	$(bb)(\bar{b}\bar{s})$		15183	~ 0
		E_{CC1}		14787				14876	
		E_{CC2}		15153				15183	
		E_{CC}		14787				14876	

TABLE VI. The average values of each operator in the Hamiltonian of the $cc\bar{c}\bar{n}$ and $bb\bar{b}\bar{n}$ tetraquark system in units of MeV. $E_{M(J/\psi D^*)}$ and $E_{M(\Upsilon B^*)}$ stand for the sum of the theoretical thresholds of $J/\psi D^*$ and ΥB^* channel, where the distance between two mesons is very large and the interactions between them are ignored.

$J^P = 2^+$		$\langle H_T \rangle$	$\langle V_{CON} \rangle$	$\langle V_{OGE} \rangle$		$\langle H_T \rangle$	$\langle V_{CON} \rangle$	$\langle V_{OGE} \rangle$
	$E_{(J/\psi D^*)^1}$	1802.8	-1812.7	-380.4	$E_{(\Upsilon B^*)^1}$	1382.6	-1328.1	-952.4
	E_{CC1}	1802.5	-1812.6	-380.3	E_{CC1}	1382.5	-1328.1	-952.4
	E_{CC2}	1994.3	-1695.1	-353.3	E_{CC2}	1594.4	-1255.3	-834.8
	E_{CC}	1801.2	-1812.7	-390.5	E_{CC}	1382.3	-1328.0	-952.3
	$E_{M(J/\psi D^*)}$	1800.1	-1812.8	-380.5	$E_{M(\Upsilon B^*)}$	1380.5	-1328.9	-953.5
	$\Delta E_{(J/\psi D^*)^1}$	2.7	0.1	0.1	$\Delta E_{(\Upsilon B^*)^1}$	2.6	0.8	1.1
	ΔE_{CC1}	2.4	0.2	0.2	ΔE_{CC1}	2.0	0.8	1.1
	ΔE_{CC2}	194.2	117.7	27.2	ΔE_{CC2}	213.9	73.6	118.7
	ΔE_{CC}	1.1	0.1	-10.0	ΔE_{CC}	1.8	0.9	1.3

B. The $QQ\bar{Q}\bar{q}$ system

In Table VII, we present our estimations of the eigenenergies of the $cc\bar{b}\bar{q}$ system with $J^P = 0^+, 1^+, \text{ and } 2^+$, respectively. For the case of the $cc\bar{b}\bar{n}$ tetraquark with $J^P = 0^+$, we find there are four meson-meson channels and

two diquark-antidiquark channels. The lowest physical threshold of $cc\bar{b}\bar{n}$ is the one of $B_c^+ D$, which is 8140 MeV. The eigenenergies obtained from the single channel, the coupled channel in each configuration, and the full coupled-channel estimations are all above the threshold

TABLE VII. The lowest-lying eigenenergies of the $cc\bar{b}\bar{n}$ $n = \{u, d\}$ and $cc\bar{b}\bar{s}$ tetraquarks in the ChQM.

J^P	$[i, j, k]$	$cc\bar{b}\bar{n}$			$cc\bar{b}\bar{s}$				
		Channel	E_{th}	E_{sc}	$P(\%)$	Channel	E_{th}	E_{sc}	$P(\%)$
0^+	[3, 1, 1]	$(B_c^+ D)^1$	8140	8142	99.42	$(B_c^+ D_s^+)^1$	8243	8244	99.94
	[3, 2, 1]	$(B_c^{*+} D^*)^1$	8307	8309	~ 0	$(B_c^{*+} D_s^+)^1$	8412	8413	~ 0
	[3, 1, 2]	$(B_c^+ D)^8$		8755	~ 0	$(B_c^+ D_s^+)^8$		8840	~ 0
	[3, 2, 2]	$(B_c^{*+} D^*)^8$		8756	~ 0	$(B_c^{*+} D_s^+)^8$		8806	~ 0
	[4, 1, 3]	$(cc)(\bar{b}\bar{n})$		8735	~ 0	$(cc)(\bar{b}\bar{s})$		8816	~ 0
	[4, 2, 4]	$(cc)(\bar{b}\bar{n})$		8657	~ 0	$(cc)(\bar{b}\bar{s})$		8728	~ 0
	E_{CC1}			8142				8244	
	E_{CC2}			8651				8719	
	E_{CC}			8142				8244	
	1^+	[3, 3, 1]	$(B_c^+ D^*)^1$	8282	8284	~ 0	$(B_c^+ D_s^{*+})^1$	8387	8388
[3, 4, 1]		$(B_c^{*+} D)^1$	8165	8167	98.00	$(B_c^{*+} D_s^+)^1$	8268	8269	99.91
[3, 5, 1]		$(B_c^{*+} D^*)^1$	8307	8309	~ 0	$(B_c^{*+} D_s^{*+})^1$	8412	8413	~ 0
[3, 3, 2]		$(B_c^+ D^*)^8$		8734	~ 0	$(B_c^+ D_s^{*+})^8$		8818	~ 0
[3, 4, 2]		$(B_c^{*+} D)^8$		8749	~ 0	$(B_c^{*+} D_s^+)^8$		8833	~ 0
[3, 5, 2]		$(B_c^{*+} D^*)^8$		8739	~ 0	$(B_c^{*+} D_s^{*+})^8$		8806	~ 0
[4, 3, 3]		$(cc)(\bar{b}\bar{n})$		8724	~ 0	$(cc)(\bar{b}\bar{s})$		8804	~ 0
[4, 4, 4]		$(cc)(\bar{b}\bar{n})$		8644	~ 0	$(cc)(\bar{b}\bar{s})$		8717	~ 0
[4, 5, 4]		$(cc)(\bar{b}\bar{n})$		8662	~ 0	$(cc)(\bar{b}\bar{s})$		8735	~ 0
E_{CC1}				8166				8269	
E_{CC2}			8640				8710		
E_{CC}			8166				8269		
2^+	[3, 6, 1]	$(B_c^{*+} D^*)^1$	8307	8309	99.75	$(B_c^{*+} D_s^{*+})^1$	8412	8413	99.96
	[3, 6, 2]	$(B_c^+ D^*)^8$		8719	~ 0	$(B_c^+ D_s^{*+})^8$		8818	~ 0
	[4, 6, 4]	$(cc)(\bar{b}\bar{n})$		8671	~ 0	$(cc)(\bar{b}\bar{s})$		8747	~ 0
	E_{CC1}			8309				8413	
	E_{CC2}			8719				8747	
	E_{CC}			8308				8413	

of $B_c^+ D$. From the full coupled-channel estimations, one can find that the dominant component of the $cc\bar{b}\bar{n}$ tetraquark state with $J^P = 0^+$ is $B_c^+ D$. As for the $cc\bar{b}\bar{n}$ tetraquark states with $J^P = 1^+$, there are six meson-meson and three diquark-antidiquark channels, respectively. The lowest physical threshold is the one of $B_c^+ D^*$, which is 8282 MeV. Similar to the case of 0^+ , the eigenenergies obtained from the single channel, the coupled channel in each configuration, and the full coupled-channel estimations are all above the threshold of $B_c^+ D^*$. Similarly, there are two meson-meson and one diquark-antidiquark channels in the $cc\bar{b}\bar{n}$ tetraquark system with $J^P = 2^+$, and our estimations also indicate that there is no below-threshold $cc\bar{b}\bar{n}$ tetraquark state with $J^P = 2^+$. Similarly, we can analyze the $cc\bar{b}\bar{s}$ tetraquark system, and we find that all the eigenenergies of the $cc\bar{b}\bar{s}$ tetraquark are above the lowest thresholds of the corresponding physical channels.

As for the $bb\bar{c}\bar{q}$ tetraquark system, the estimated eigenenergies are listed in Table VIII. For the $bb\bar{c}\bar{n}$ tetraquark states with $J^P = 0^+$, we find that the lowest threshold of physical channel is the one of $B_c^- \bar{B}$, which is 11554 MeV. The eigenenergies obtained from the

single-channel estimations and coupled-channel estimations in each configuration are above the threshold of $B_c^- \bar{B}$. While considering the coupled-channel effects of meson-meson and diquark-antidiquark configurations simultaneously, we find that the eigenenergy of the $bb\bar{c}\bar{n}$ tetraquark with $J^P = 0^+$ is 11552 MeV, which is about 2 MeV below the threshold of $B_c^- \bar{B}$. In this tetraquark state, the dominant component is $B_c^- \bar{B}$, and its percentage is about 94.25. As for the $bb\bar{c}\bar{n}$ tetraquark states with $J^P = 1^+$, the lowest physical channel is $B_c^- \bar{B}^*$ with the threshold 11579 MeV. We find that the eigenenergies obtained from single-channel estimations and coupled-channel estimations in each configuration are all above the threshold of $B_c^- \bar{B}^*$, while the full coupled-channel estimations indicate that the eigenenergy of the $bb\bar{c}\bar{n}$ tetraquark states with $J^P = 1^+$ is 11566 MeV, which is about 13 MeV below the threshold of $B_c^- \bar{B}^*$. In this tetraquark state, the dominant component is $B_c^- \bar{B}^*$, and its percentage is about 58.26, while the $(B_c^- \bar{B}^*)^1$ and $(B_c^- \bar{B}^*)^8$ channels in the meson-meson configuration and $(bb)(\bar{c}\bar{n})$ channel with $[i, j, k] = [4, 4, 4]$ in the diquark-antidiquark configuration are also important with

TABLE VIII. The lowest-lying eigenenergies of the $bb\bar{c}\bar{n}$ $n = \{u, d\}$ and $bb\bar{c}\bar{s}$ tetraquarks in the ChQM.

J^P	$[i, j, k]$	$bb\bar{c}\bar{n}$				$bb\bar{c}\bar{s}$				
		Channel	E_{th}	E_{sc}	$P(\%)$	Channel	E_{th}	E_{sc}	$P(\%)$	
0^+	[3, 1, 1]	$(B_c^- \bar{B})^1$	11554	11557	94.25	$(B_c^- \bar{B}_s)^1$	11642	11643	99.75	
	[3, 2, 1]	$(B_c^{*-} \bar{B}^*)^1$	11625	11627	1.45	$(B_c^{*-} \bar{B}_s^*)^1$	11715	11716	~ 0	
	[3, 1, 2]	$(B_c^- \bar{B})^8$		12003	~ 0	$(B_c^- \bar{B}_s)^8$		12062	~ 0	
	[3, 2, 2]	$(B_c^{*-} \bar{B}^*)^8$		12082	1.24	$(B_c^{*-} \bar{B}_s^*)^8$		12114	~ 0	
	[4, 1, 3]	$(bb)(\bar{c}\bar{n})$		12146	~ 0	$(bb)(\bar{c}\bar{s})$		12193	~ 0	
	[4, 2, 4]	$(bb)(\bar{c}\bar{n})$		11827	2.31	$(bb)(\bar{c}\bar{s})$		11893	~ 0	
	E_{CC1}			11556				11643		
	E_{CC2}			11826				11893		
	E_{CC}			11552				11643		
	1^+	[3, 3, 1]	$(B_c^- \bar{B}^*)^1$	11600	11602	15.71	$(B_c^- \bar{B}_s^*)^1$	11690	11691	~ 0
		[3, 4, 1]	$(B_c^{*-} \bar{B})^1$	11579	11582	58.26	$(B_c^{*-} \bar{B}_s)^1$	11667	11668	98.59
[3, 5, 1]		$(B_c^{*-} \bar{B}^*)^1$	11625	11627	~ 0	$(B_c^{*-} \bar{B}_s^*)^1$	11715	11716	~ 0	
[3, 3, 2]		$(B_c^- \bar{B}^*)^8$		11987	~ 0	$(B_c^- \bar{B}_s^*)^8$		12043	~ 0	
[3, 4, 2]		$(B_c^{*-} \bar{B})^8$		11990	~ 0	$(B_c^{*-} \bar{B}_s)^8$		12046	~ 0	
[3, 5, 2]		$(B_c^{*-} \bar{B}^*)^8$		12010	6.16	$(B_c^{*-} \bar{B}_s^*)^8$		12050	~ 0	
[4, 3, 3]		$(bb)(\bar{c}\bar{n})$		12110	1.58	$(bb)(\bar{c}\bar{s})$		12157	~ 0	
[4, 4, 4]		$(bb)(\bar{c}\bar{n})$		11759	16.57	$(bb)(\bar{c}\bar{s})$		11827	~ 0	
[4, 5, 4]		$(bb)(\bar{c}\bar{n})$		11828	~ 0	$(bb)(\bar{c}\bar{s})$		11896	~ 0	
E_{CC1}				11581				11668		
E_{CC2}				11759				11826		
E_{CC}			11566				11668			
2^+	[3, 6, 1]	$(B_c^{*-} \bar{B}^*)^1$	11625	11627	68.00	$(B_c^{*-} \bar{B}_s^*)^1$	11715	11716	99.57	
	[3, 6, 2]	$(B_c^- \bar{B}^*)^8$		11961	9.79	$(B_c^- \bar{B}_s^*)^8$		12031	~ 0	
	[4, 6, 4]	$(bb)(\bar{c}\bar{n})$		11833	22.21	$(bb)(\bar{c}\bar{s})$		11901	~ 0	
	E_{CC1}			11626				11716		
	E_{CC2}			11833				11901		
	E_{CC}			11613				11716		

the percentage 15.71, 6.16, and 16.57, respectively. For the $J^P = 2^+$ case, there is only one physical channel for the $bb\bar{c}\bar{n}$ tetraquark state, which is $B_c^{*-} \bar{B}^*$ with the threshold 11625 MeV. Similar to the case of 0^+ and 2^+ , the eigenenergies obtained from the single-channel estimations and the coupled-channel estimations in each configuration are all above the threshold of $B_c^{*-} \bar{B}^*$. When we consider both meson-meson and diquark-antidiquark configurations simultaneously, the eigenenergy of the $bb\bar{c}\bar{n}$ tetraquark state with $J^P = 2^+$ is estimated to be 11613 MeV, which is about 12 MeV below the threshold of $B_c^{*-} \bar{B}^*$, and the percentage of different channels is 68.00, 9.79, and 22.21 for $(B_c^{*-} \bar{B}^*)^1$, $(B_c^- \bar{B}^*)^8$, and $(bb)(\bar{c}\bar{n})$ channels with $[i, j, k] = [4, 6, 4]$, respectively. Different from the $bb\bar{c}\bar{n}$ tetraquark system, our estimations indicate that the eigenenergies of $bb\bar{c}\bar{s}$ tetraquark states with different J^P quantum numbers are all above the lowest threshold of the corresponding physical channels.

From our estimations, we find there is no below-threshold $QQ\bar{Q}'\bar{s}$ tetraquark state. But for the $QQ\bar{Q}'\bar{n}$ tetraquark system, we find that the eigenenergies of all the S -wave ground $bb\bar{c}\bar{n}$ tetraquark states with different J^P

quantum numbers are below the lowest threshold of the corresponding physical channels, which is much different with the $cc\bar{b}\bar{n}$ case. To further compare the spectrum of $cc\bar{b}\bar{n}$ and $bb\bar{c}\bar{n}$, we list the average values of each operator in the Hamiltonian of the tetraquark systems in Table IX. It is interesting to notice that in the full coupled-channel estimation all the eigenenergies of the $bb\bar{c}\bar{n}$ tetraquark states are below the corresponding lowest physical threshold, while the eigenenergies of the $cc\bar{b}\bar{n}$ are all above the corresponding lowest physical threshold. By comparing the average values of the operators in the Hamiltonian of the $cc\bar{b}\bar{n}$ and $bb\bar{c}\bar{n}$ tetraquark system, one finds the dominant difference is the average values of V_{OGE} , especially in the case of coupled-channel estimations in the diquark-antidiquark configurations. The average values of V_{OGE} are negative, which indicates that the OGE potential is attractive. However, for the $cc\bar{b}\bar{n}$ tetraquark states with $J^P = 0^+$ and 2^+ , the attractions become weak when we consider coupled-channel effects in each configuration, and, for the $J^P = 2^+$ case, the attraction becomes stronger in the diquark-antidiquark coupled-channel estimations. For the $bb\bar{c}\bar{n}$ tetraquark states, we find that the attractions

TABLE IX. The same as Table VI but for $cc\bar{b}\bar{n}$ and $bb\bar{c}\bar{n}$ tetraquark states with $J^P = 0^+, 1^+, \text{ and } 2^+$.

		$\langle H_T \rangle$	$\langle V_{\text{CON}} \rangle$	$\langle V_{\text{OGE}} \rangle$		$\langle H_T \rangle$	$\langle V_{\text{CON}} \rangle$	$\langle V_{\text{OGE}} \rangle$
$J^P = 0^+$	$E_{(B_c^+ D)^1}$	1662.7	-1984.5	-416.5	$E_{(B_c^- \bar{B})^1}$	1522.7	-1880.4	-349.9
	E_{CC1}	1662.4	-1985.2	-416.2	E_{CC1}	1522.4	-1882.7	-348.9
	E_{CC2}	1861.4	-1751.3	-339.7	E_{CC2}	1698.3	-1550.5	-586.6
	E_{CC}	1660.3	-1984.9	-414.6	E_{CC}	1521.2	-1882.8	-351.3
	$E_{M(B_c^+ D)}$	1660.2	-1984.6	-416.6	$E_{M(B_c^- \bar{B})}$	1519.3	-1880.3	-350.0
	$\Delta E_{(B_c^+ D)^1}$	2.5	0.1	0.1	$\Delta E_{(B_c^- \bar{B})^1}$	3.5	-0.1	0.1
	ΔE_{CC1}	2.2	-0.6	0.4	ΔE_{CC1}	3.1	-2.4	1.1
	ΔE_{CC2}	201.2	233.3	76.9	ΔE_{CC2}	179.0	329.8	-236.6
	ΔE_{CC}	0.1	-0.3	2.0	ΔE_{CC}	2.0	-2.8	-1.3
	$J^P = 1^+$	$E_{(B_c^{*+} D)^1}$	1662.7	-1984.5	-391.5	$E_{(B_c^{*-} \bar{B})^1}$	1522.7	-1880.4
E_{CC1}		1662.3	-1985.3	-391.2	E_{CC1}	1521.9	-1883.5	-322.8
E_{CC2}		1851.2	-1741.1	-351.0	E_{CC2}	1695.4	-1548.2	-652.8
E_{CC}		1662.4	-1985.3	-391.2	E_{CC}	1520.3	-1884.9	-334.5
$E_{M(B_c^{*+} D)}$		1660.2	-1984.5	-391.6	$E_{M(B_c^{*-} \bar{B})}$	1519.3	-1880.3	-325.0
$\Delta E_{(B_c^{*+} D)^1}$		2.5	0.0	0.1	$\Delta E_{(B_c^{*-} \bar{B})^1}$	3.4	-0.1	0.1
ΔE_{CC1}		2.1	-0.8	0.4	ΔE_{CC1}	2.6	-3.2	2.2
ΔE_{CC2}		197.0	243.4	40.6	ΔE_{CC2}	176.1	332.1	-327.8
ΔE_{CC}		2.2	-0.8	0.4	ΔE_{CC}	1.0	-4.6	-9.5
$J^P = 2^+$		$E_{(B_c^{*+} D^{*})^1}$	1662.7	-1984.5	-249.5	$E_{(B_c^{*-} B^{*})^1}$	1522.7	-1880.4
	E_{CC1}	1662.7	-1985.1	-249.4	E_{CC1}	1522.7	-1881.9	-279.8
	E_{CC2}	1839.2	-1728.8	-319.9	E_{CC2}	1694.0	-1547.0	-579.4
	E_{CC}	1661.5	-1983.8	-249.9	E_{CC}	1521.8	-1883.5	-289.7
	$E_{M(B_c^{*+} D^{*})}$	1660.2	-1984.5	-249.6	$E_{M(B_c^{*-} B^{*})}$	1520.4	-1880.3	-280.0
	$\Delta E_{(B_c^{*+} D^{*})^1}$	2.5	0.0	0.1	$\Delta E_{(B_c^{*-} B^{*})^1}$	2.3	-0.1	0.1
	ΔE_{CC1}	2.5	0.4	0.2	ΔE_{CC1}	2.3	-1.6	0.2
	ΔE_{CC2}	179.0	255.7	-70.4	ΔE_{CC2}	173.6	333.3	-299.4
	ΔE_{CC}	1.3	0.7	-0.3	ΔE_{CC}	1.2	-3.2	-9.7

become much stronger in the diquark-antidiquark coupled-channel estimations, although the attractions caused by the confinement potential become weak and the eigenenergies obtained in the diquark-antidiquark coupled-channel estimations are still above the corresponding lowest physical threshold. But when we consider the coupled-channel effects in both configurations, the eigenenergies of the $bb\bar{c}\bar{n}$ are below the corresponding lowest threshold of the physical channels.

C. The $QQ'\bar{Q}\bar{q}$ system

Similar to the cases of $QQ\bar{Q}'\bar{q}$ and $QQ'\bar{Q}\bar{q}$ tetraquark states, we can estimate the eigenenergies of $QQ'\bar{Q}\bar{q}$ tetraquark states. Our estimations of the eigenenergies of the $cb\bar{c}\bar{q}$ and $bc\bar{b}\bar{q}$ tetraquark states are collected in Tables X and XI. From Table X, one can find that the eigenenergies of the $bc\bar{c}\bar{n}$ tetraquark state with $J^P = 0^+$ obtained in the single-channel estimations, the coupled-channel estimations in each configuration, and the full coupled-channel estimations are all above the threshold of DB_c^- , which is 8140 MeV. Similarly, we also find that the eigenenergies of the $bc\bar{c}\bar{s}$ tetraquark states with $J^P = 0^+$

are all above the threshold of $D_s^+ B_c^-$. As for the $bc\bar{c}\bar{n}$ tetraquark state with $J^P = 1^+$, we find that the eigenenergies obtained in the single-channel estimations and the coupled-channel estimations in the meson-meson and diquark-antidiquark configurations are all above the threshold of DB_c^{*-} ; however, when considering the coupled-channel effects in both meson-meson and diquark-antidiquark configurations, one obtains the eigenenergy to be 8159 MeV, which is 6 MeV below the threshold of DB_c^{*-} . In this tetraquark state, the dominant component is DB_c^{*-} with a percentage to be 91.57. As for the $bc\bar{c}\bar{s}$ tetraquark state with $J^P = 1^+$, we find that the eigenenergies obtained in the single-channel estimations, the coupled-channel estimations in each configuration, and the full coupled-channel estimations are all above the threshold of $D_s^+ B_c^{*-}$. As for the case of $J^P = 2^+$, the eigenenergies of $bc\bar{c}\bar{n}$ and $bc\bar{c}\bar{s}$ obtained in the full coupled-channel estimations are 8273 and 8410 MeV, which are below the threshold of $D^* B_c^{*-}$ and $D_s^{*+} B_c^{*-}$, respectively. In the $bc\bar{b}\bar{n}$ tetraquark state with $J^P = 2^+$, the dominant components are $(D^* B_c^{*-})^1$, $(J/\psi B^*)^8$, and $(bc)(\bar{c}\bar{n})$ with $[i, j, k] = [7, 6, 4]$; the corresponding

TABLE X. The lowest-lying eigenenergies of the $bc\bar{c}\bar{n}$ $n = \{u, d\}$ and $bc\bar{c}\bar{s}$ tetraquarks in the ChQM.

J^P	$[i, j, k]$	$bc\bar{c}\bar{n}$			$bc\bar{c}\bar{s}$				
		Channel	E_{th}	E_{sc}	$P(\%)$	Channel	E_{th}	E_{sc}	$P(\%)$
0^+	[5, 1, 1]	$(\eta_c \bar{B})^1$	8266	8266	~ 0	$(\eta_c \bar{B}_s)^1$	8351	8352	~ 0
	[5, 2, 1]	$(J/\psi \bar{B}^*)^1$	8422	8424	~ 0	$(J/\psi \bar{B}_s^*)^1$	8512	8513	~ 0
	[5, 1, 2]	$(\eta_c \bar{B})^8$		8717	~ 0	$(\eta_c \bar{B}_s)^8$		8796	~ 0
	[5, 2, 2]	$(J/\psi \bar{B}^*)^8$		8663	~ 0	$(J/\psi \bar{B}_s^*)^8$		8733	~ 0
	[6, 1, 1]	$(DB_c^-)^1$	8140	8142	98.94	$(D_s^+ B_c^-)^1$	8243	8244	99.92
	[6, 2, 1]	$(D^* B_c^{*-})^1$	8307	8309	~ 0	$(D_s^{*+} B_c^{*-})^1$	8412	8413	~ 0
	[6, 1, 2]	$(DB_c^-)^8$		8870	~ 0	$(D_s^+ B_c^-)^8$		8924	~ 0
	[6, 2, 2]	$(D^* B_c^{*-})^8$		8815	~ 0	$(D_s^{*+} B_c^{*-})^8$		8860	~ 0
	[7, 1, 3]	$(bc)(\bar{c}\bar{n})$		8864	~ 0	$(bc)(\bar{c}\bar{s})$		8924	~ 0
	[7, 1, 4]	$(bc)(\bar{c}\bar{n})$		8648	~ 0	$(bc)(\bar{c}\bar{s})$		8722	~ 0
	[7, 2, 3]	$(bc)(\bar{c}\bar{n})$		8864	~ 0	$(bc)(\bar{c}\bar{s})$		8924	~ 0
	[7, 2, 4]	$(bc)(\bar{c}\bar{n})$		8643	~ 0	$(bc)(\bar{c}\bar{s})$		8715	~ 0
		E_{CC1}		8141				8244	
		E_{CC2}		8647				8711	
		E_{CC}		8141				8244	
1^+	[5, 3, 1]	$(\eta_c \bar{B}^*)^1$	8309	8311	~ 0	$(\eta_c \bar{B}_s^*)^1$	8399	8400	~ 0
	[5, 4, 1]	$(J/\psi \bar{B})^1$	8377	8379	~ 0	$(J/\psi \bar{B}_s)^1$	8464	8465	~ 0
	[5, 5, 1]	$(J/\psi \bar{B}^*)^1$	8422	8424	~ 0	$(J/\psi \bar{B}_s^*)^1$	8512	8513	~ 0
	[5, 3, 2]	$(\eta_c \bar{B}^*)^8$		8711	~ 0	$(\eta_c \bar{B}_s^*)^8$		8790	~ 0
	[5, 4, 2]	$(J/\psi \bar{B})^8$		8702	~ 0	$(J/\psi \bar{B}_s)^8$		8781	~ 0
	[5, 5, 2]	$(J/\psi \bar{B}^*)^8$		8680	1.77	$(J/\psi \bar{B}_s^*)^8$		8754	~ 0
	[6, 3, 1]	$(DB_c^{*-})^1$	8165	8167	91.57	$(D_s^+ B_c^{*-})^1$	8268	8269	99.76
	[6, 4, 1]	$(D^* B_c^-)^1$	8282	8284	~ 0	$(D_s^{*+} B_c^-)^1$	8387	8388	~ 0
	[6, 5, 1]	$(D^* B_c^{*-})^1$	8307	8309	~ 0	$(D_s^{*+} B_c^{*-})^1$	8412	8413	~ 0
	[6, 3, 2]	$(DB_c^{*-})^8$		8867	~ 0	$(D_s^+ B_c^{*-})^8$		8921	~ 0
	[6, 4, 2]	$(D^* B_c^-)^8$		8853	~ 0	$(D_s^{*+} B_c^-)^8$		8906	~ 0
	[6, 5, 2]	$(D^* B_c^{*-})^8$		8833	~ 0	$(D_s^{*+} B_c^{*-})^8$		8882	~ 0
	[7, 3, 3]	$(bc)(\bar{c}\bar{n})$		8828	~ 0	$(bc)(\bar{c}\bar{s})$		8888	~ 0
	[7, 3, 4]	$(bc)(\bar{c}\bar{n})$		8640	~ 0	$(bc)(\bar{c}\bar{s})$		8715	~ 0
	[7, 4, 3]	$(bc)(\bar{c}\bar{n})$		8858	~ 0	$(bc)(\bar{c}\bar{s})$		8918	~ 0
	[7, 4, 4]	$(bc)(\bar{c}\bar{n})$		8582	1.17	$(bc)(\bar{c}\bar{s})$		8656	~ 0
	[7, 5, 3]	$(bc)(\bar{c}\bar{n})$		8803	~ 0	$(bc)(\bar{c}\bar{s})$		8722	~ 0
	[7, 5, 4]	$(bc)(\bar{c}\bar{n})$		8648	1.19	$(bc)(\bar{c}\bar{s})$		8858	~ 0
	E_{CC1}		8167				8269		
	E_{CC2}		8554				8633		
	E_{CC}		8159				8269		
2^+	[5, 6, 1]	$(J/\psi \bar{B}^*)^1$	8422	8424	~ 0	$(J/\psi \bar{B}_s^*)^1$	8512	8513	~ 0
	[6, 6, 1]	$(J/\psi \bar{B}^*)^8$		8713	11.04	$(J/\psi \bar{B}_s^*)^8$		8796	1.59
	[5, 6, 2]	$(D^* B_c^{*-})^1$	8307	8309	72.10	$(D_s^{*+} B_c^{*-})^1$	8412	8413	95.29
	[6, 6, 2]	$(D^* B_c^{*-})^8$		8866	1.38	$(D_s^{*+} B_c^{*-})^8$		8924	~ 0
	[7, 6, 3]	$(bc)(\bar{c}\bar{n})$		8841	4.53	$(bc)(\bar{c}\bar{s})$		8906	~ 0
	[7, 6, 4]	$(bc)(\bar{c}\bar{n})$		8657	10.77	$(bc)(\bar{c}\bar{s})$		8734	1.94
		E_{CC1}		8308				8413	
		E_{CC2}		8623				8708	
	E_{CC}		8273				8410		

percentages of these components are 72.10, 11.04, and 10.77, respectively. As for the $bc\bar{b}\bar{s}$ tetraquark state with $J^P = 2^+$, the dominant component is $(D_s^{*+} B_c^{*-})^1$ with a percentage of 95.29.

As for the $bc\bar{b}\bar{q}$ tetraquark system, the eigenenergies estimated in the ChQM are collected in Table XI. From the table, one can find that the eigenenergies obtained in the single-channel estimations, coupled-channel estimations in

TABLE XI. The lowest-lying eigenenergies of the $bc\bar{b}\bar{n}$ $n = \{u, d\}$ and $bc\bar{b}\bar{s}$ tetraquarks in the ChQM.

J^P	$[i, j, k]$	$bc\bar{b}\bar{n}$			$bc\bar{b}\bar{s}$				
		Channel	E_{th}	E_{sc}	$P(\%)$	Channel	E_{th}	E_{sc}	$P(\%)$
0^+	[5, 1, 1]	$(\eta_b D_s^+)^1$	11264	11266	99.99	$(\eta_b D_s^+)^1$	11367	11368	99.99
	[5, 2, 1]	$(\Upsilon D_s^*)^1$	11467	11469	~ 0	$(\Upsilon D_s^{*+})^1$	11572	11573	~ 0
	[5, 1, 2]	$(\eta_b D_s^+)^8$		12085	~ 0	$(\eta_b D_s^+)^1)^8$		12135	~ 0
	[5, 2, 2]	$(\Upsilon D_s^*)^8$		12050	~ 0	$(\Upsilon D_s^{*+})^8$		12094	~ 0
	[6, 1, 1]	$(\bar{B} B_c^+)^1$	11555	11557	~ 0	$(\bar{B}_s B_c^+)^1$	11642	11643	~ 0
	[6, 2, 1]	$(\bar{B}^* B_c^{*+})^1$	11625	11627	~ 0	$(\bar{B}_s^* B_c^{*+})^1$	11715	11716	~ 0
	[6, 1, 2]	$(\bar{B} B_c^+)^8$		12002	~ 0	$(\bar{B}_s B_c^+)^8$		12035	~ 0
	[6, 2, 2]	$(\bar{B}^* B_c^{*+})^8$		11957	~ 0	$(\bar{B}_s^* B_c^{*+})^8$		11982	~ 0
	[7, 1, 3]	$(bc)(\bar{b}\bar{n})$		12039	~ 0	$(bc)(\bar{b}\bar{s})$		12077	~ 0
	[7, 1, 4]	$(bc)(\bar{b}\bar{n})$		11899	~ 0	$(bc)(\bar{b}\bar{s})$		11951	~ 0
	[7, 2, 3]	$(bc)(\bar{b}\bar{n})$		11989	~ 0	$(bc)(\bar{b}\bar{s})$		12018	~ 0
	[7, 2, 4]	$(bc)(\bar{b}\bar{n})$		11925	~ 0	$(bc)(\bar{b}\bar{s})$		11976	~ 0
		E_{CC1}		11266				11368	
		E_{CC2}		11879				11912	
		E_{CC}		11266				11368	
1^+	[5, 3, 1]	$(\eta_b D_s^{*+})^1$	11406	11408	~ 0	$(\eta_b D_s^{*+})^1$	11511	11512	$\sim 0\%$
	[5, 4, 1]	$(\Upsilon D_s^+)^1$	11325	11327	99.99	$(\Upsilon D_s^+)^1$	11428	11429	99.99%
	[5, 5, 1]	$(\Upsilon D_s^*)^1$	11467	11433	~ 0	$(\Upsilon D_s^{*+})^1$	11572	11573	~ 0
	[5, 3, 2]	$(\eta_b D_s^+)^8$		12067	~ 0	$(\eta_b D_s^+)^8$		12117	~ 0
	[5, 4, 2]	$(\Upsilon D_s^+)^8$		12082	~ 0	$(\Upsilon D_s^+)^8$		12131	~ 0
	[5, 5, 2]	$(\Upsilon D_s^*)^8$		12057	~ 0	$(\Upsilon D_s^{*+})^8$		12104	~ 0
	[6, 3, 1]	$(\bar{B} B_c^{*+})^1$	11580	11582	~ 0	$(\bar{B}_s B_c^{*+})^1$	11667	11668	~ 0
	[6, 4, 1]	$(\bar{B}^* B_c^+)^1$	11600	11602	~ 0	$(\bar{B}_s^* B_c^+)^1$	11690	11691	~ 0
	[6, 5, 1]	$(\bar{B}^* B_c^{*+})^1$	11625	11627	~ 0	$(\bar{B}_s^* B_c^{*+})^1$	11715	11716	~ 0
	[6, 3, 2]	$(\bar{B} B_c^{*+})^8$		11999	~ 0	$(\bar{B}_s B_c^{*+})^8$		12032	~ 0
	[6, 4, 2]	$(\bar{B}^* B_c^+)^8$		11997	~ 0	$(\bar{B}_s^* B_c^+)^8$		12029	~ 0
	[6, 5, 2]	$(\bar{B}^* B_c^{*+})^8$		11975	~ 0	$(\bar{B}_s^* B_c^{*+})^8$		12004	~ 0
	[7, 3, 3]	$(bc)(\bar{b}\bar{n})$		12027	~ 0	$(bc)(\bar{b}\bar{s})$		12065	~ 0
	[7, 3, 4]	$(bc)(\bar{b}\bar{n})$		11921	~ 0	$(bc)(\bar{b}\bar{s})$		11975	~ 0
	[7, 4, 3]	$(bc)(\bar{b}\bar{n})$		12032	~ 0	$(bc)(\bar{b}\bar{s})$		12070	~ 0
	[7, 4, 3]	$(bc)(\bar{b}\bar{n})$		11911	~ 0	$(bc)(\bar{b}\bar{s})$		11963	~ 0
	[7, 5, 3]	$(bc)(\bar{b}\bar{n})$		12005	~ 0	$(bc)(\bar{b}\bar{s})$		12038	~ 0
	[7, 5, 4]	$(bc)(\bar{b}\bar{n})$		11929	~ 0	$(bc)(\bar{b}\bar{s})$		11981	~ 0
		E_{CC1}		11327				11429	
		E_{CC2}		11891				11926	
	E_{CC}		11327				11429		
2^+	[5, 6, 1]	$(\Upsilon D_s^*)^1$	11467	11469	99.99	$(\Upsilon D_s^{*+})^1$	11572	11573	99.99%
	[6, 6, 1]	$(\Upsilon D_s^*)^8$		12071	~ 0	$(\Upsilon D_s^{*+})^8$		12123	~ 0
	[5, 6, 2]	$(\bar{B}^* B_c^{*+})^1$	11625	11627	~ 0	$(\bar{B}_s^* B_c^{*+})^1$	11715	11716	~ 0
	[6, 6, 2]	$(\bar{B}^* B_c^{*+})^8$		12012	~ 0	$(\bar{B}_s^* B_c^{*+})^8$		12048	~ 0
	[7, 6, 3]	$(bc)(\bar{b}\bar{n})$		12037	~ 0	$(bc)(\bar{b}\bar{s})$		12078	~ 0
	[7, 6, 4]	$(bc)(\bar{b}\bar{n})$		11937	~ 0	$(bc)(\bar{b}\bar{s})$		11992	~ 0
		E_{CC1}		11469				11573	
		E_{CC2}		11930				11982	
	E_{CC}		11469				11573		

each configuration, and the full coupled-channel estimations are all above the corresponding lowest physical threshold, which is different with the $bc\bar{c}\bar{q}$ tetraquark states, where one finds three below-threshold tetraquark

states. To further analyze the role of the coupled-channel effects, we estimate the average values of the operators in the Hamiltonian of the $Q'Q\bar{Q}\bar{q}$ system, which are collected in Tables XII and XIII. From the tables, one can find that

TABLE XII. Contributions of each term in the Hamiltonian to the energy of the $bc\bar{c}\bar{n}$ tetraquark and $bc\bar{b}\bar{n}$ tetraquark in ChQM. $E_{M(\text{“channel”})}$ stands for the sum of the theoretical thresholds of the lowest physical channel (unit, MeV).

		$\langle H_T \rangle$	$\langle V_{\text{CON}} \rangle$	$\langle V_{\text{OGE}} \rangle$		$\langle H_T \rangle$	$\langle V_{\text{CON}} \rangle$	$\langle V_{\text{OGE}} \rangle$
$J^P = 1^+$	$E_{(DB_c^-)^1}$	1662.7	-1984.6	-391.6	$E_{(\Upsilon D)^1}$	1558.6	-1432.2	-1064.1
	E_{CC1}	1661.9	-1985.3	-391.0	E_{CC1}	1558.4	-1432.2	-1063.9
	E_{CC2}	1856.1	-1870.1	-312.9	E_{CC2}	1772.2	-1534.8	-610.9
	E_{CC}	1661.2	-1998.9	-384.0	E_{CC}	1558.0	-1432.1	-1063.7
	$E_{M(DB_c^-)}$	1660.2	-1984.6	-391.6	$E_{M(\Upsilon D)}$	1556.6	-1432.9	-1064.1
	$\Delta E_{(DB_c^-)^1}$	2.5	0.0	0.0	$\Delta E_{(\Upsilon D)^1}$	2.0	0.7	0.0
	ΔE_{CC1}	1.7	-0.7	0.6	ΔE_{CC1}	1.8	0.7	0.2
	ΔE_{CC2}	195.9	114.5	78.7	ΔE_{CC2}	215.6	-101.9	453.2
	ΔE_{CC}	1.0	-14.3	7.6	ΔE_{CC}	1.4	0.8	-0.6
$J^P = 2^+$	$E_{(D^*B_c^-)^1}$	1662.7	-1984.6	-249.6	$E_{(\Upsilon D^*)^1}$	1558.4	-1432.2	-922.1
	E_{CC1}	1660.9	-1984.9	-249.1	E_{CC1}	1558.2	-1432.1	-921.9
	E_{CC2}	1852.5	-1875.3	-234.4	E_{CC2}	1724.6	-1637.5	-421.6
	E_{CC}	1660.3	-1998.9	-269.8	E_{CC}	1557.7	-1431.8	-921.3
	$E_{M(D^*B_c^-)}$	1660.2	-1984.6	-249.6	$E_{M(\Upsilon D^*)}$	1556.6	-1432.9	-922.8
	$\Delta E_{(D^*B_c^-)^1}$	2.5	0.0	0.0	$\Delta E_{(\Upsilon D^*)^1}$	1.8	0.7	0.7
	ΔE_{CC1}	0.7	-0.3	0.5	ΔE_{CC1}	1.6	0.8	0.8
	ΔE_{CC2}	192.3	109.3	15.2	ΔE_{CC2}	168.0	-204.4	501.2
	ΔE_{CC}	0.1	-14.3	-20.2	ΔE_{CC}	1.8	0.7	1.5

TABLE XIII. Contributions of each term in Hamiltonian to the energy of the $bc\bar{c}\bar{s}$ and $bc\bar{b}\bar{s}$ tetraquark in ChQM. $E_{M(\text{“channel”})}$ stands for the sum of the theoretical thresholds of the lowest physical channel (unit, MeV).

		$\langle H_T \rangle$	$\langle V_{\text{CON}} \rangle$	$\langle V_{\text{OGE}} \rangle$		$\langle H_T \rangle$	$\langle V_{\text{CON}} \rangle$	$\langle V_{\text{OGE}} \rangle$
$J^P = (2^+)$	$E_{(D_s^{*+}B_c^-)^1}$	1176.7	-1474.3	-392.6	$E_{(\Upsilon D_s^{*+})^1}$	1036.7	-921.9	-1065.1
	E_{CC1}	1176.3	-1475.0	-392.3	E_{CC1}	1036.5	-921.9	-1065.0
	E_{CC2}	1347.7	-1396.2	-347.2	E_{CC2}	1231.6	-1100.5	-636.5
	E_{CC}	1176.1	-1478.2	-391.9	E_{CC}	1036.5	-921.9	-1064.9
	$E_{M(D_s^{*+}B_c^-)}$	1174.9	-1474.2	-392.5	$E_{M(\Upsilon D_s^{*+})}$	1036.4	-922.2	-1065.6
	$\Delta E_{(D_s^{*+}B_c^-)^1}$	1.8	-0.1	-0.1	$\Delta E_{(\Upsilon D_s^{*+})^1}$	0.3	0.3	0.5
	ΔE_{CC1}	1.4	-0.8	0.2	ΔE_{CC1}	0.1	0.3	0.6
	ΔE_{CC2}	172.8	78.0	45.3	ΔE_{CC2}	195.2	-278.3	430.1
	ΔE_{CC}	1.2	-4.0	0.6	ΔE_{CC}	0.1	0.3	0.7

the average values of kinetic terms increase when we include the interaction between mesons and coupled-channel effects. In the full coupled-channel estimations, we find that the attraction from confinement potential becomes stronger for $bc\bar{c}\bar{n}$ tetraquark states with $J^P = 1^+$ and $J^P = 2^+$, but the attraction from the OGE potential becomes weak for the $bc\bar{c}\bar{n}$ tetraquark states with $J^P = 1^+$, while this attraction becomes strong for the $bc\bar{c}\bar{n}$ tetraquark states with $J^P = 2^+$. As for $bc\bar{c}\bar{s}$ tetraquark states, the full coupled-channel estimations indicate that the average values of H_T , V_{CON} , and V_{OGE} are close to those of $E_{M(\Upsilon D)}$, and the sum of these terms is positive. As for the $bc\bar{c}\bar{s}$ tetraquark state with $J^P = 2^+$, the estimations indicate that the confinement potential becomes strong in the full coupled-channel estimation.

V. SUMMARY

In summary, inspired by the recent observation of fully heavy tetraquark states, we perform a systematic estimation of the triply tetraquark states in a chiral quark model, where the coupled-channel effects of meson-meson and diquark-antidiquark configurations are included. The eigenenergies of the S -wave ground states have been estimated. After including the coupled-channel effects of both configurations, we notice that the eigenenergies of some tetraquark states are below the corresponding lowest threshold of the physical channel, which indicates that these tetraquark states cannot fall apart directly and, thus, are stable for strong decay. In Table XIV, we collect all the stable tetraquark states estimated in the present work. For

TABLE XIV. Possible bound states with different quantum numbers in ChQM (unit, MeV).

J^P	Quark components	E_{th}	E_{cc}	B_{cc}
2^+	$cc\bar{c}\bar{n}$	5104	5095	-9
0^+	$bb\bar{c}\bar{n}$	11554	11552	-2
1^+	$bb\bar{c}\bar{n}$	11579	11566	-13
2^+	$bb\bar{c}\bar{n}$	11625	11613	-12
1^+	$bc\bar{c}\bar{n}$	8165	8159	-6
2^+	$bc\bar{c}\bar{n}$	8307	8273	-34
2^+	$bc\bar{c}\bar{s}$	8412	8410	-2

comparison, we also list the corresponding lowest thresholds of the physical channel.

Moreover, comparing with the results in Refs. [126–128,130], we find that the masses of the diquark-antidiquark configurations are several hundred MeV higher than those of the color-magnetic interaction model [126,128] and QCD sum rules [127], while the masses under an extended relativized quark model [130] are generally consistent with present estimations of the diquark-diquark configurations. Although there are discrepancies in the estimated masses due to different input parameters and different interactions in different models, the conclusions are basically the same for the triply heavy tetraquark system; i.e., no stable states are found in the diquark-antidiquark configurations except for the estimation of QCD sum rules [127]. But when we consider the coupled-channel effects of diquark-antidiquark and meson-meson configurations simultaneously, we find there exist several stable tetraquark states which are below the corresponding lowest physical threshold, which may be accessible for experiments in LHCb.

ACKNOWLEDGMENTS

This work is supported partly by the National Natural Science Foundation of China under Contracts No. 12175037, No. 11775050, No. 11775118, and No. 11535005, and this work is also supported by China Postdoctoral Science Foundation funded Projects No. 2021M690626 and No. 1107020201 and the Fundamental Research Funds for the Central Universities No. 2242022R20040.

APPENDIX: THE WAVE FUNCTION OF THE TRIPLY HEAVY TETRAQUARK

1. The color wave function

For the meson-meson configurations, the color wave functions of a $q\bar{q}$ cluster are

$$\begin{aligned}
C_{[111]}^1 &= \sqrt{\frac{1}{3}}(r\bar{r} + g\bar{g} + b\bar{b}), \\
C_{[21]}^2 &= r\bar{b}, & C_{[21]}^3 &= -r\bar{g}, \\
C_{[21]}^4 &= g\bar{b}, & C_{[21]}^5 &= -b\bar{g}, \\
C_{[21]}^6 &= g\bar{r}, & C_{[21]}^7 &= b\bar{r}, \\
C_{[21]}^8 &= \sqrt{\frac{1}{2}}(r\bar{r} - g\bar{g}), \\
C_{[21]}^9 &= \sqrt{\frac{1}{6}}(-r\bar{r} - g\bar{g} + 2b\bar{b}), \tag{A1}
\end{aligned}$$

where the subscripts [111] and [21] stand for color singlet ($\mathbf{1}_c$) and color octet ($\mathbf{8}_c$), respectively. Then the color-singlet tetraquark $SU(3)_{\text{color}}$ wave functions can be constructed by two color-singlet clusters, i.e., $\mathbf{1}_c \otimes \mathbf{1}_c$, and by two color-octet clusters, i.e., $\mathbf{8}_c \otimes \mathbf{8}_c$, which are

$$\begin{aligned}
\chi_1^c &= C_{[111]}^1 C_{[111]}^1, \\
\chi_2^c &= \sqrt{\frac{1}{8}} \left(C_{[21]}^2 C_{[21]}^7 - C_{[21]}^4 C_{[21]}^5 - C_{[21]}^3 C_{[21]}^6 \right. \\
&\quad \left. + C_{[21]}^8 C_{[21]}^8 - C_{[21]}^6 C_{[21]}^3 + C_{[21]}^9 C_{[21]}^9 \right. \\
&\quad \left. - C_{[21]}^5 C_{[21]}^4 + C_{[21]}^7 C_{[21]}^2 \right). \tag{A2}
\end{aligned}$$

For the diquark-antidiquark configuration, the color wave functions of the diquark clusters are

$$\begin{aligned}
C_{[2]}^1 &= rr, & C_{[2]}^2 &= \sqrt{\frac{1}{2}}(rg + gr), \\
C_{[2]}^3 &= gg, & C_{[2]}^4 &= \sqrt{\frac{1}{2}}(rb + br), \\
C_{[2]}^5 &= \sqrt{\frac{1}{2}}(gb + bg), & C_{[2]}^6 &= bb, \\
C_{[11]}^7 &= \sqrt{\frac{1}{2}}(rg - gr), & C_{[11]}^8 &= \sqrt{\frac{1}{2}}(rb - br), \\
C_{[11]}^9 &= \sqrt{\frac{1}{2}}(gb - bg). \tag{A3}
\end{aligned}$$

The color wave functions of the antidiquark clusters are

$$\begin{aligned}
C_{[22]}^1 &= \bar{r}\bar{r}, & C_{[22]}^2 &= -\sqrt{\frac{1}{2}}(\bar{r}\bar{g} + \bar{g}\bar{r}), \\
C_{[22]}^3 &= \bar{g}\bar{g}, & C_{[22]}^4 &= \sqrt{\frac{1}{2}}(\bar{r}\bar{b} + \bar{b}\bar{r}), \\
C_{[22]}^5 &= -\sqrt{\frac{1}{2}}(\bar{g}\bar{b} + \bar{b}\bar{g}), & C_{[22]}^6 &= \bar{b}\bar{b}, \\
C_{[211]}^7 &= \sqrt{\frac{1}{2}}(\bar{r}\bar{g} - \bar{g}\bar{r}), & C_{[211]}^8 &= -\sqrt{\frac{1}{2}}(\bar{r}\bar{b} - \bar{b}\bar{r}), \\
C_{[211]}^9 &= \sqrt{\frac{1}{2}}(\bar{g}\bar{b} - \bar{b}\bar{g}). & & \quad (\text{A4})
\end{aligned}$$

The color-singlet wave functions of the diquark-antidiquark configuration can be the product of color sextet and antisextet clusters ($\mathbf{6}_c \otimes \bar{\mathbf{6}}_c$) or the product of color triplet and antitriplet cluster ($\mathbf{6}_c \otimes \bar{\mathbf{6}}_c$), which read

$$\begin{aligned}
\chi_3^c &= \sqrt{\frac{1}{6}}(C_{[2]}^1 C_{[22]}^1 - C_{[2]}^2 C_{[22]}^{[2]} + C_{[2]}^3 C_{[22]}^3 \\
&\quad + C_{[2]}^4 C_{[22]}^4 - C_{[2]}^5 C_{[22]}^5 + C_{[2]}^6 C_{[22]}^6), \\
\chi_4^c &= \sqrt{\frac{1}{3}}(C_{[11]}^7 C_{[211]}^7 - C_{[11]}^8 C_{[211]}^8 + C_{[11]}^9 C_{[211]}^9). \quad (\text{A5})
\end{aligned}$$

2. The flavor wave function

For the flavor degree of freedom, the quark content of the investigated four-quark system is $QQ\bar{Q}\bar{q}$, $Q = \{c, b\}$, $q = \{u, d, s\}$, and the isospin could be 1/2 and 0. Here, we adopt F_m^i and F_d^i to denote the flavor wave functions of the tetraquark system in the meson-meson and diquark-antidiquark configurations, respectively. In the present work, the flavor wave function of the $QQ\bar{Q}\bar{q}$ system can be categorized into three types, which are $QQ\bar{Q}\bar{q}$, $QQ\bar{Q}'\bar{q}$, and $QQ'\bar{Q}\bar{q}$, respectively.

For the $QQ\bar{Q}\bar{q}$ system, the flavor wave functions can be

$$F_m^1 = (Q\bar{Q})(Q\bar{q}), \quad F_d^2 = (QQ)(\bar{Q}\bar{q}), \quad (\text{A6})$$

and, for the $QQ\bar{Q}'\bar{q}$ system, the flavor wave functions can be read as

$$F_m^3 = (Q\bar{Q}')(Q\bar{q}), \quad F_d^4 = (QQ)(\bar{Q}'\bar{q}). \quad (\text{A7})$$

The flavor wave functions for the $QQ'\bar{Q}\bar{q}$ system read

$$\begin{aligned}
F_m^5 &= (Q\bar{Q})(Q'\bar{q}), \\
F_m^6 &= (Q\bar{q})(Q'\bar{Q}), \\
F_d^7 &= (QQ')(Q\bar{q}). \quad (\text{A8})
\end{aligned}$$

3. The spin wave function

The total spin S of tetraquark states can be 0, 1, and 2. The spin wave functions of two-body clusters are

$$\begin{aligned}
\chi_{11} &= \alpha\alpha, \\
\chi_{10} &= \sqrt{\frac{1}{2}}(\alpha\beta + \beta\alpha), \\
\chi_{1-1} &= \beta\beta, \\
\chi_{00} &= \sqrt{\frac{1}{2}}(\alpha\beta - \beta\alpha). \quad (\text{A9})
\end{aligned}$$

Then, the spin wave functions of the tetraquark state S_s^i can be constructed by considering the coupling of two sub-cluster spin wave functions with SU(2) algebra, which read

$$\begin{aligned}
S_0^1 &= \chi_{00}\chi_{00}, \\
S_0^2 &= \sqrt{\frac{1}{3}}(\chi_{11}\chi_{1-1} - \chi_{10}\chi_{10} + \chi_{1-1}\chi_{11}), \\
S_1^3 &= \chi_{00}\chi_{11}, \\
S_1^4 &= \chi_{11}\chi_{00}, \\
S_1^5 &= \sqrt{\frac{1}{2}}(\chi_{11}\chi_{10} - \chi_{10}\chi_{11}), \\
S_2^6 &= \chi_{11}\chi_{11}. \quad (\text{A10})
\end{aligned}$$

[1] H. X. Chen, W. Chen, X. Liu, and S. L. Zhu, *Phys. Rep.* **639**, 1 (2016).
[2] E. S. Swanson, *Phys. Rep.* **429**, 243 (2006).
[3] M. B. Voloshin, *Prog. Part. Nucl. Phys.* **61**, 455 (2008).
[4] R. Chen, X. Liu, and S. L. Zhu, *Nucl. Phys.* **A954**, 406 (2016).
[5] A. Esposito, A. Pilloni, and A. D. Polosa, *Phys. Rep.* **668**, 1 (2017).

[6] R. F. Lebed, R. E. Mitchell, and E. S. Swanson, *Prog. Part. Nucl. Phys.* **93**, 143 (2017).
[7] F. K. Guo, C. Hanhart, U. G. Meißner, Q. Wang, Q. Zhao, and B. S. Zou, *Rev. Mod. Phys.* **90**, 015004 (2018).
[8] M. Gell-Mann, *Phys. Lett.* **8**, 214 (1964).
[9] S. K. Choi *et al.* (Belle Collaboration), *Phys. Rev. Lett.* **91**, 262001 (2003).
[10] B. Aubert *et al.* (BABAR Collaboration), *Phys. Rev. Lett.* **90**, 242001 (2003).

- [11] D. Besson *et al.* (CLEO Collaboration), *Phys. Rev. D* **68**, 032002 (2003); **75**, 119908(E) (2007).
- [12] P. Krokovny *et al.* (Belle Collaboration), *Phys. Rev. Lett.* **91**, 262002 (2003).
- [13] S. Godfrey, *Phys. Lett. B* **568**, 254 (2003).
- [14] J. L. Rosner, *J. Phys. G* **34**, S127 (2007).
- [15] J. Liu, Q. Wu, J. He, D. Y. Chen, and T. Matsuki, *Phys. Rev. D* **101**, 014003 (2020).
- [16] S. Godfrey and N. Isgur, *Phys. Rev. D* **32**, 189 (1985).
- [17] C. J. Xiao, D. Y. Chen, and Y. L. Ma, *Phys. Rev. D* **93**, 094011 (2016).
- [18] T. Barnes, F. E. Close, and H. J. Lipkin, *Phys. Rev. D* **68**, 054006 (2003).
- [19] F. S. Navarra, M. Nielsen, E. Oset, and T. Sekihara, *Phys. Rev. D* **92**, 014031 (2015).
- [20] E. E. Kolomeitsev and M. F. M. Lutz, *Phys. Lett. B* **582**, 39 (2004).
- [21] J. Hofmann and M. F. M. Lutz, *Nucl. Phys. A* **733**, 142 (2004).
- [22] F. K. Guo, P. N. Shen, H. C. Chiang, R. G. Ping, and B. S. Zou, *Phys. Lett. B* **641**, 278 (2006).
- [23] Y. J. Zhang, H. C. Chiang, P. N. Shen, and B. S. Zou, *Phys. Rev. D* **74**, 014013 (2006).
- [24] J. L. Rosner, *Phys. Rev. D* **74**, 076006 (2006).
- [25] F. K. Guo, P. N. Shen, and H. C. Chiang, *Phys. Lett. B* **647**, 133 (2007).
- [26] H. Y. Cheng and W. S. Hou, *Phys. Lett. B* **566**, 193 (2003).
- [27] Y. Q. Chen and X. Q. Li, *Phys. Rev. Lett.* **93**, 232001 (2004).
- [28] H. Kim and Y. Oh, *Phys. Rev. D* **72**, 074012 (2005).
- [29] M. Nielsen, R. D. Matheus, F. S. Navarra, M. E. Bracco, and A. Lozea, *Nucl. Phys. B, Proc. Suppl.* **161**, 193 (2006).
- [30] K. Terasaki, arXiv:hep-ph/0512285.
- [31] Z. G. Wang and S. L. Wan, *Nucl. Phys. A* **778**, 22 (2006).
- [32] D. Acosta *et al.* (CDF Collaboration), *Phys. Rev. Lett.* **93**, 072001 (2004).
- [33] A. Abulencia *et al.* (CDF Collaboration), *Phys. Rev. Lett.* **96**, 102002 (2006).
- [34] A. Abulencia *et al.* (CDF Collaboration), *Phys. Rev. Lett.* **98**, 132002 (2007).
- [35] T. Aaltonen *et al.* (CDF Collaboration), *Phys. Rev. Lett.* **103**, 152001 (2009).
- [36] V. M. Abazov *et al.* (D0 Collaboration), *Phys. Rev. Lett.* **93**, 162002 (2004).
- [37] B. Aubert *et al.* (BABAR Collaboration), *Phys. Rev. Lett.* **93**, 041801 (2004).
- [38] B. Aubert *et al.* (BABAR Collaboration), *Phys. Rev. D* **71**, 071103 (2005).
- [39] B. Aubert *et al.* (BABAR Collaboration), *Phys. Rev. D* **71**, 052001 (2005).
- [40] B. Aubert *et al.* (BABAR Collaboration), *Phys. Rev. D* **73**, 011101 (2006).
- [41] B. Aubert *et al.* (BABAR Collaboration), *Phys. Rev. Lett.* **96**, 052002 (2006).
- [42] B. Aubert *et al.* (BABAR Collaboration), *Phys. Rev. D* **74**, 071101 (2006).
- [43] B. Aubert *et al.* (BABAR Collaboration), *Phys. Rev. D* **77**, 011102 (2008).
- [44] B. Aubert *et al.* (BABAR Collaboration), *Phys. Rev. D* **77**, 111101 (2008).
- [45] B. Aubert *et al.* (BABAR Collaboration), *Phys. Rev. Lett.* **102**, 132001 (2009).
- [46] P. del Amo Sanchez *et al.* (BABAR Collaboration), *Phys. Rev. D* **82**, 011101 (2010).
- [47] CMS Collaboration, Report No. CMS-PAS-BPH-10-018.
- [48] A. Vesentini (CMS Collaboration), *Nuovo Cimento C* **035**, 21 (2012).
- [49] S. Chatrchyan *et al.* (CMS Collaboration), *J. High Energy Phys.* **04** (2013) 154.
- [50] M. Dall’Osso (CMS Collaboration), *Proc. Sci. Beauty2013* (2013) 066.
- [51] M. Dall’Osso (CMS Collaboration), *Nuovo Cimento C* **037**, 283 (2014).
- [52] A. M. Sirunyan *et al.* (CMS Collaboration), *Phys. Rev. Lett.* **125**, 152001 (2020).
- [53] R. Aaij *et al.* (LHCb Collaboration), *Eur. Phys. J. C* **72**, 1972 (2012).
- [54] LHCb Collaboration, Report Nos. LHCb-CONF-2011-043, CERN-LHCb-CONF-2011-043.
- [55] LHCb Collaboration, Report Nos. LHCb-CONF-2011-021, CERN-LHCb-CONF-2011-021.
- [56] R. Aaij *et al.* (LHCb Collaboration), *Phys. Rev. Lett.* **110**, 222001 (2013).
- [57] R. Aaij *et al.* (LHCb Collaboration), *Eur. Phys. J. C* **73**, 2462 (2013).
- [58] R. Aaij *et al.* (LHCb Collaboration), *Nucl. Phys.* **B886**, 665 (2014).
- [59] R. Aaij *et al.* (LHCb Collaboration), *Phys. Rev. D* **92**, 011102 (2015).
- [60] R. Aaij *et al.* (LHCb Collaboration), *Phys. Lett. B* **769**, 305 (2017).
- [61] R. Aaij *et al.* (LHCb Collaboration), *Eur. Phys. J. C* **77**, 609 (2017).
- [62] R. Aaij *et al.* (LHCb Collaboration), *J. High Energy Phys.* **09** (2019) 028.
- [63] J. Matthew Durham (LHCb Collaboration), *Nucl. Phys.* **A1005**, 121918 (2021).
- [64] R. Aaij *et al.* (LHCb Collaboration), *Phys. Rev. D* **102**, 092005 (2020).
- [65] R. Aaij *et al.* (LHCb Collaboration), *J. High Energy Phys.* **08** (2020) 123.
- [66] R. Aaij *et al.* (LHCb Collaboration), *J. High Energy Phys.* **02** (2021) 024.
- [67] M. Ablikim *et al.* (BESIII Collaboration), *Phys. Rev. Lett.* **112**, 092001 (2014).
- [68] M. Ablikim *et al.* (BESIII Collaboration), *Phys. Rev. Lett.* **122**, 202001 (2019).
- [69] M. Ablikim *et al.* (BESIII Collaboration), *Phys. Rev. Lett.* **122**, 232002 (2019).
- [70] M. Ablikim *et al.* (BESIII Collaboration), *Phys. Rev. Lett.* **124**, 242001 (2020).
- [71] T. Barnes and S. Godfrey, *Phys. Rev. D* **69**, 054008 (2004).
- [72] E. J. Eichten, K. Lane, and C. Quigg, *Phys. Rev. D* **69**, 094019 (2004).
- [73] Y. Chen *et al.* (CLQCD Collaboration), arXiv: hep-lat/0701021.
- [74] X. Liu and Y. M. Wang, *Eur. Phys. J. C* **49**, 643 (2007).
- [75] T. H. Wang and G. L. Wang, *Phys. Lett. B* **697**, 233 (2011).
- [76] Y. S. Kalashnikova and A. V. Nefediev, *Phys. Rev. D* **82**, 097502 (2010).

- [77] T. Wang, G. L. Wang, Y. Jiang, and W. L. Ju, *J. Phys. G* **40**, 035003 (2013).
- [78] C. Meng and K. T. Chao, *Phys. Rev. D* **75**, 114002 (2007).
- [79] Y. R. Liu and Z. Y. Zhang, *Phys. Rev. C* **79**, 035206 (2009).
- [80] D. Gamermann and E. Oset, *Phys. Rev. D* **80**, 014003 (2009).
- [81] M. B. Voloshin and L. B. Okun, *Pis'ma Zh. Eksp. Teor. Fiz.* **23**, 369 (1976); [*JETP Lett.* **23**, 333 (1976)], <https://inspirehep.net/literature/113708>.
- [82] A. De Rujula, H. Georgi, and S. L. Glashow, *Phys. Rev. Lett.* **38**, 317 (1977).
- [83] N. A. Tornqvist, *Z. Phys. C* **61**, 525 (1994).
- [84] C. E. Thomas and F. E. Close, *Phys. Rev. D* **78**, 034007 (2008).
- [85] I. W. Lee, A. Faessler, T. Gutsche, and V. E. Lyubovitskij, *Phys. Rev. D* **80**, 094005 (2009).
- [86] X. Chen, B. Wang, X. Li, X. Zeng, S. Yu, and X. Lu, *Phys. Rev. D* **79**, 114006 (2009).
- [87] D. Gamermann, J. Nieves, E. Oset, and E. Ruiz Arriola, *Phys. Rev. D* **81**, 014029 (2010).
- [88] P. G. Ortega, J. Segovia, D. R. Entem, and F. Fernandez, *AIP Conf. Proc.* **1257**, 331 (2010).
- [89] F. K. Guo, C. Hidalgo-Duque, J. Nieves, and M. P. Valderrama, *Phys. Rev. D* **88**, 054007 (2013).
- [90] P. Wang and X. G. Wang, *Phys. Rev. Lett.* **111**, 042002 (2013).
- [91] C. Y. Wong, *Phys. Rev. C* **69**, 055202 (2004).
- [92] E. S. Swanson, *Phys. Lett. B* **588**, 189 (2004).
- [93] J. Vijande, F. Fernandez, and A. Valcarce, *Int. J. Mod. Phys. A* **20**, 702 (2005).
- [94] L. Maiani, V. Riquer, F. Piccinini, and A. D. Polosa, *Phys. Rev. D* **72**, 031502 (2005).
- [95] F. S. Navarra and M. Nielsen, *Phys. Lett. B* **639**, 272 (2006).
- [96] Y. Cui, X. L. Chen, W. Z. Deng, and S. L. Zhu, *High Energy Phys. Nucl. Phys.* **31**, 7 (2007), [arXiv:hep-ph/0607226](https://arxiv.org/abs/hep-ph/0607226).
- [97] R. D. Matheus, S. Narison, M. Nielsen, and J. M. Richard, *Phys. Rev. D* **75**, 014005 (2007).
- [98] M. Nielsen, F. S. Navarra, and M. E. Bracco, *Braz. J. Phys.* **37**, 56 (2007).
- [99] S. Dubnicka, A. Z. Dubnickova, M. A. Ivanov, and J. G. Korner, *Phys. Rev. D* **81**, 114007 (2010).
- [100] S. Dubnicka, A. Z. Dubnickova, M. A. Ivanov, J. G. Koerner, P. Santorelli, and G. G. Saidullaeva, *Phys. Rev. D* **84**, 014006 (2011).
- [101] D. Ebert, R. N. Faustov, and V. O. Galkin, *Phys. Lett. B* **634**, 214 (2006).
- [102] L. Maiani, F. Piccinini, A. D. Polosa, and V. Riquer, *Phys. Rev. D* **71**, 014028 (2005).
- [103] Z. G. Wang and T. Huang, *Phys. Rev. D* **89**, 054019 (2014).
- [104] F. E. Close and S. Godfrey, *Phys. Lett. B* **574**, 210 (2003).
- [105] B. A. Li, *Phys. Lett. B* **605**, 306 (2005).
- [106] A. A. Petrov, *J. Phys. Conf. Ser.* **9**, 83 (2005).
- [107] LHCb Collaboration, *Sci. Bull.* **65**, 1983 (2020).
- [108] K. Y. on behalf of the CMS Collaboration, <https://agenda.infn.it/event/28874/contributions/170300/>.
- [109] E. B.-T. on behalf of the ATLAS Collaboration, <https://agenda.infn.it/event/28874/contributions/170298/>.
- [110] R. M. Albuquerque, S. Narison, A. Rabemananjara, D. Rabetiarivony, and G. Randriamanatrika, *Phys. Rev. D* **102**, 094001 (2020).
- [111] M. S. Liu, F. X. Liu, X. H. Zhong, and Q. Zhao, [arXiv:2006.11952](https://arxiv.org/abs/2006.11952).
- [112] Q. F. Lü, D. Y. Chen, and Y. B. Dong, *Eur. Phys. J. C* **80**, 871 (2020).
- [113] J. F. Giron and R. F. Lebed, *Phys. Rev. D* **102**, 074003 (2020).
- [114] H. G. Dosch, S. J. Brodsky, G. F. de T eramond, M. Nielsen, and L. Zou, *Nucl. Part. Phys. Proc.* **312–317**, 135 (2021).
- [115] B. C. Yang, L. Tang, and C. F. Qiao, *Eur. Phys. J. C* **81**, 324 (2021).
- [116] G. Huang, J. Zhao, and P. Zhuang, *Phys. Rev. D* **103**, 054014 (2021).
- [117] B. D. Wan and C. F. Qiao, *Phys. Lett. B* **817**, 136339 (2021).
- [118] J. W. Zhu, X. D. Guo, R. Y. Zhang, W. G. Ma, and X. Q. Li, [arXiv:2011.07799](https://arxiv.org/abs/2011.07799).
- [119] Z. H. Guo and J. A. Oller, *Phys. Rev. D* **103**, 034024 (2021).
- [120] X. K. Dong, V. Baru, F. K. Guo, C. Hanhart, and A. Nefediev, *Phys. Rev. Lett.* **126**, 132001 (2021); **127**, 119901(E) (2021).
- [121] C. Gong, M. C. Du, Q. Zhao, X. H. Zhong, and B. Zhou, *Phys. Lett. B* **824**, 136794 (2022).
- [122] J. Z. Wang, D. Y. Chen, X. Liu, and T. Matsuki, *Phys. Rev. D* **103**, 071503 (2021).
- [123] J. Z. Wang and X. Liu, *Phys. Rev. D* **106**, 054015 (2022).
- [124] C. Gong, M. C. Du, and Q. Zhao, *Phys. Rev. D* **106**, 054011 (2022).
- [125] Z. R. Liang and D. L. Yao, *Rev. Mex. Fis. Suppl.* **3**, 0308042 (2022).
- [126] K. Chen, X. Liu, J. Wu, Y. R. Liu, and S. L. Zhu, *Eur. Phys. J. A* **53**, 5 (2017).
- [127] J. F. Jiang, W. Chen, and S. L. Zhu, *Phys. Rev. D* **96**, 094022 (2017).
- [128] X. Z. Weng, W. Z. Deng, and S. L. Zhu, *Phys. Rev. D* **105**, 034026 (2022).
- [129] B. Silvestre-Brac and C. Semay, *Z. Phys. C* **57**, 273 (1993).
- [130] Q. F. Lü, D. Y. Chen, Y. B. Dong, and E. Santopinto, *Phys. Rev. D* **104**, 054026 (2021).
- [131] A. Valcarce, H. Garcilazo, F. Fernandez, and P. Gonzalez, *Rep. Prog. Phys.* **68**, 965 (2005).
- [132] J. Segovia, A. M. Yasser, D. R. Entem, and F. Fernandez, *Phys. Rev. D* **78**, 114033 (2008).
- [133] J. Segovia, D. R. Entem, and F. Fernandez, *J. Phys. G* **37**, 075010 (2010).
- [134] J. Segovia, D. R. Entem, F. Fernandez, and E. Ruiz Arriola, *Phys. Rev. D* **85**, 074001 (2012).
- [135] J. Segovia, P. G. Ortega, D. R. Entem, and F. Fern andez, *Phys. Rev. D* **93**, 074027 (2016).
- [136] J. Segovia, C. Albertus, D. R. Entem, F. Fernandez, E. Hernandez, and M. A. Perez-Garcia, *Phys. Rev. D* **84**, 094029 (2011).

- [137] J. Segovia, D. R. Entem, and F. Fernandez, *Phys. Rev. D* **83**, 114018 (2011).
- [138] J. Segovia, D. R. Entem, and F. Fernández, *Phys. Lett. B* **715**, 322 (2012).
- [139] J. Segovia, D. R. Entem, and F. Fernandez, *Nucl. Phys. A* **915**, 125 (2013).
- [140] J. Segovia, D. R. Entem, and F. Fernández, *Phys. Rev. D* **91**, 014002 (2015).
- [141] P. G. Ortega, J. Segovia, D. R. Entem, and F. Fernandez, *Phys. Rev. D* **81**, 054023 (2010).
- [142] P. G. Ortega, J. Segovia, D. R. Entem, and F. Fernández, *Phys. Rev. D* **94**, 114018 (2016).
- [143] X. Jin, Y. Xue, H. Huang, and J. Ping, *Eur. Phys. J. C* **80**, 1083 (2020).
- [144] Y. Yan, Y. Wu, X. Hu, H. Huang, and J. Ping, *Phys. Rev. D* **105**, 014027 (2022).
- [145] X. Liu, H. Huang, J. Ping, and D. Chen, *Phys. Rev. C* **103**, 025202 (2021).
- [146] X. Jin, Y. Xue, H. Huang, and J. Ping, *Eur. Phys. J. C* **80**, 1083 (2020).
- [147] X. Liu, H. Huang, and J. Ping, *Phys. Rev. C* **98**, 055203 (2018).
- [148] X. Liu, D. Chen, H. Huang, J. Ping, X. Chen, and Y. Yang, *Sci. China Phys. Mech. Astron.* **66**, 221012 (2023).
- [149] M. Tanabashi *et al.* (Particle Data Group), *Phys. Rev. D* **98**, 030001 (2018).
- [150] M. Kamimura, *Nucl. Phys. A* **351**, 456 (1981).